



Severe hypoxaemic hypercapnia compounds cerebral oxidative–nitrosative stress during extreme apnoea: Implications for cerebral bioenergetic function

Davison, G., Bailey, D., Bain, A., Hoiland, R., Barak, O., Drvis, I., Stacey, B., Iannetelli, A., Davison, G., Dahl, R., Berg, R., MacLeod, D., Dujic, Z., & Ainslie, P. (2024). Severe hypoxaemic hypercapnia compounds cerebral oxidative–nitrosative stress during extreme apnoea: Implications for cerebral bioenergetic function. *Journal of Physiology*, 1-26. Advance online publication. <https://doi.org/10.1113/JP285555>

[Link to publication record in Ulster University Research Portal](#)

Published in:
Journal of Physiology

Publication Status:
Published online: 13/02/2024







DOI:
[10.1113/JP285555](https://doi.org/10.1113/JP285555)

Document Version
Publisher's PDF, also known as Version of record

General rights
Copyright for the publications made accessible via Ulster University's Research Portal is retained by the author(s) and / or other copyright owners and it is a condition of accessing these publications that users recognise and abide by the legal requirements associated with these rights.

Take down policy
The Research Portal is Ulster University's institutional repository that provides access to Ulster's research outputs. Every effort has been made to ensure that content in the Research Portal does not infringe any person's rights, or applicable UK laws. If you discover content in the Research Portal that you believe breaches copyright or violates any law, please contact pure-support@ulster.ac.uk.

Severe hypoxaemic hypercapnia compounds cerebral oxidative–nitrosative stress during extreme apnoea: Implications for cerebral bioenergetic function

Damian M. Bailey¹ , Anthony R. Bain² , Ryan L. Hoiland^{3,4}, Otto F. Barak^{5,6}, Ivan Drvis⁷, Benjamin S. Stacey¹ , Angelo Iannetelli¹, Gareth W. Davison⁸, Rasmus H. Dahl⁹ , Ronan M. G. Berg^{1,10}, David B. MacLeod¹¹ , Zeljko Dujic⁵ and Philip N. Ainslie^{1,12} 

¹Neurovascular Research Laboratory, Faculty of Life Sciences and Education, University of South Wales, Glamorgan, UK

²Department of Kinesiology, Faculty of Human Kinetics, University of Windsor, Windsor, ON, Canada

³Department of Anaesthesiology, Pharmacology and Therapeutics, Vancouver General Hospital, West 12th Avenue, University of British Columbia, Vancouver, BC, Canada

⁴Department of Cellular and Physiological Sciences, Faculty of Medicine, University of British Columbia, Vancouver, BC, Canada

⁵Department of Integrative Physiology, School of Medicine, University of Split, Split, Croatia

⁶Department of Sports Medicine, Faculty of Medicine, University of Novi Sad, Novi Sad, Serbia

⁷School of Kinesiology, University of Zagreb, Zagreb, Croatia

⁸Department of Exercise Biochemistry and Physiology, Sport and Exercise Science Research Institute, Ulster University Belfast, United Kingdom of Great Britain and Northern Ireland, Ulster, UK

⁹Department of Radiology, University Hospital Rigshospitalet, Copenhagen, Denmark

¹⁰Department of Biomedical Sciences, University of Copenhagen, Denmark

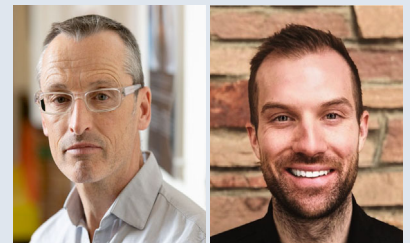
¹¹Department of Anesthesiology, Duke University Medical Center, Durham, NC, USA

¹²School of Health and Exercise Sciences, Faculty of Health and Social Development, Center for Heart Lung and Vascular Health, University of British Columbia, Kelowna, BC, Canada

Handling Editors: Harold Schultz & Igor Fernandes

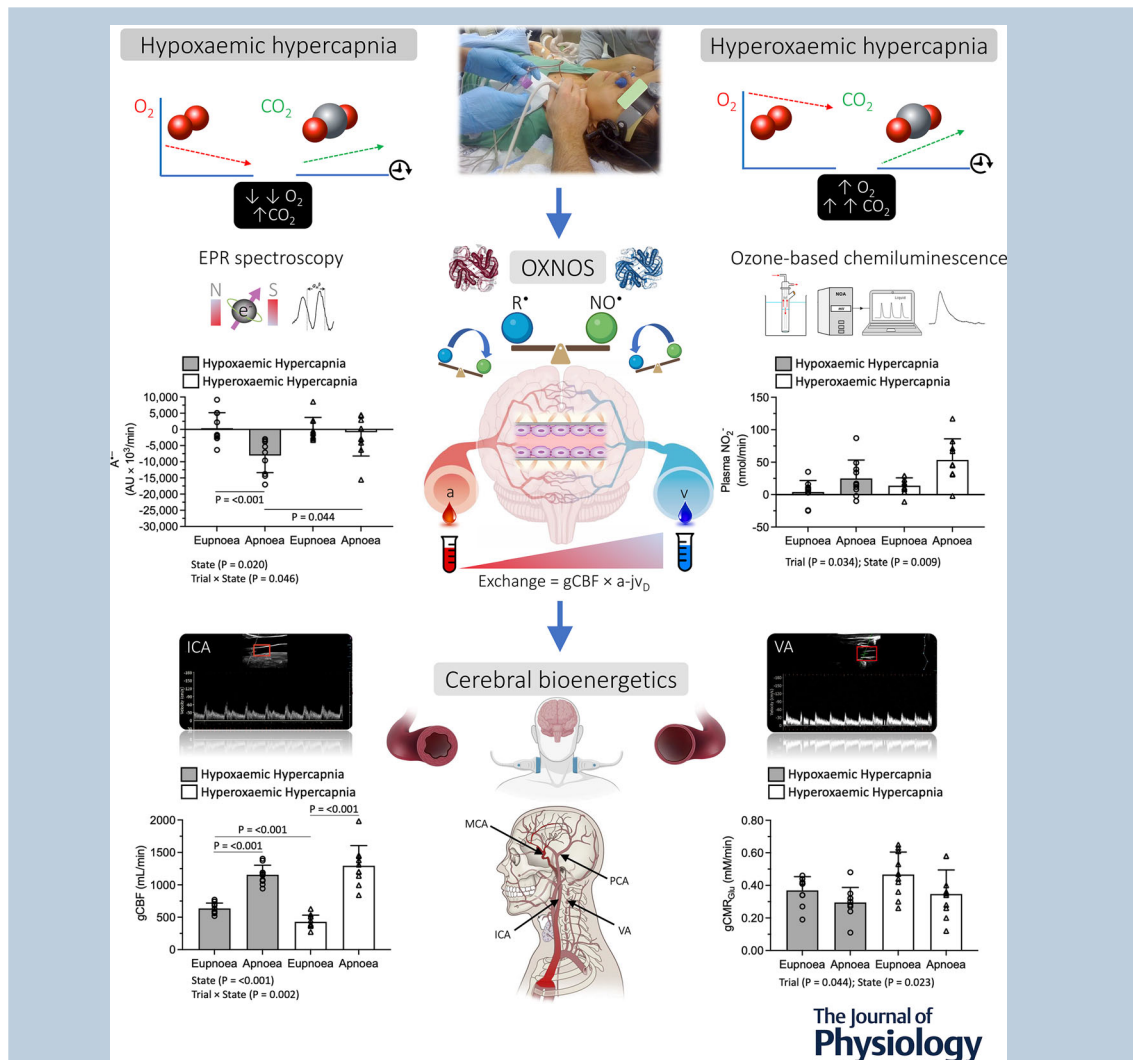
The peer review history is available in the Supporting information section of this article (<https://doi.org/10.1113/JP285555#support-information-section>).

Damian M. Bailey is a Royal Society Wolfson Research Fellow and Professor of Physiology and Biochemistry at the University of South Wales, where he leads the Neurovascular Research Laboratory. He is Editor-in-Chief of *Experimental Physiology* and Chair of the Life Sciences Working Group to the European Space Agency. His research programme takes an integrative translational approach to investigate how free radicals and associated reactive oxygen/nitrogen species impact cerebral bioenergetic function across the clinical spectrum of human health and disease. **Anthony R. Bain** is an associate professor at the University of Windsor, Department of Kinesiology, adjunct in Integrative Biology, where he leads the Integrative Vascular Physiology Laboratory. His research programme specializes in the endothelial and cerebrovascular responses to stress, including heat, hypoxia and exercise.



Z. Dujic and P. N. Ainslie contributed equally to this work.

This article was first published as a preprint. Bailey DM, Bain AR, Hoiland RL, Barak OF, Drvis I, Stacey BS, Iannetelli A, Davison GW, Dahl RH, Berg RMG, MacLeod DB, Dujic Z, Ainslie PN. 2023. Systemic hypoxemia catalyzes cerebral oxidative-nitrosative stress during extreme apnea in humans: implications for cerebral bioenergetic function. bioRxiv. <https://doi.org/10.1101/2023.07.24.23293124>



Abstract We examined the extent to which apnoea-induced extremes of oxygen demand/carbon dioxide production impact redox regulation of cerebral bioenergetic function. Ten ultra-elite apnoeists (six men and four women) performed two maximal dry apnoeas preceded by normoxic normoventilation, resulting in severe end-apnoea hypoxaemic hypercapnia, and hyperoxic hyper-ventilation designed to ablate hypoxaemia, resulting in hyperoxaemic hypercapnia. Transcerebral exchange of ascorbate radicals (by electron paramagnetic resonance spectroscopy) and nitric oxide metabolites (by tri-iodide chemiluminescence) were calculated as the product of global cerebral blood flow (by duplex ultrasound) and radial arterial (a) to internal jugular venous (v) concentration gradients. Apnoea duration increased from 306 ± 62 s during hypoxaemic hypercapnia to 959 ± 201 s in hyperoxaemic hypercapnia ($P \leq 0.001$). Apnoea generally increased global cerebral blood flow (all $P \leq 0.001$) but was insufficient to prevent a reduction in the cerebral metabolic rates of oxygen and glucose ($P = 0.015$ – 0.044). This was associated with a general net cerebral output ($v > a$) of ascorbate radicals that was greater in hypoxaemic hypercapnia ($P = 0.046$ vs. hyperoxaemic hypercapnia) and coincided with a selective suppression in plasma nitrite uptake ($a > v$) and global cerebral blood flow ($P = 0.034$ to <0.001 vs. hyperoxaemic hypercapnia), implying reduced consumption and delivery of nitric oxide consistent with elevated cerebral oxidative–nitrosative stress. In contrast, we failed to observe equidirectional gradients consistent with S-nitrosohaemoglobin consumption and plasma S-nitrosothiol delivery during apnoea (all $P \geq 0.05$). Collectively, these findings highlight a key catalytic role for hypoxaemic hypercapnia in cerebral oxidative–nitrosative stress.

(Received 25 August 2023; accepted after revision 16 January 2024; first published online 10 February 2024)

Corresponding author D. M. Bailey: Neurovascular Research Laboratory, Alfred Russel Wallace Building, Faculty of Life Sciences and Education, University of South Wales, Glamorgan CF37 4AT, UK. Email: damian.bailey@southwales.ac.uk

Abstract figure legend We determined how physiological extremes of O₂ and CO₂ impact redox regulation of cerebral bioenergetic function. World-class breath-hold divers performed two maximal apnoeas resulting in hypoxaemic hypercapnia (prior normoxic normoventilation) and hyperoxaemic hypercapnia (prior hyperoxic hyperventilation). Trans-cerebral exchange of ascorbate free radicals (A^{•-}) and nitric oxide metabolites were calculated as the product of global cerebral blood flow (gCBF) and radial arterial (a) to internal jugular venous (v) concentration gradients. Cerebral output (v > a) of A^{•-} was enhanced in hypoxaemic hypercapnia and coincided with greater suppression of plasma nitrite (NO₂⁻) uptake (a > v), gCBF and cerebral metabolic rate of glucose (gCMR_{Glu}), implying reduced consumption and delivery of NO consistent with elevated cerebral oxidative–nitrosative stress (OXNOS). Abbreviations: ICA, internal carotid artery; MCA, middle cerebral artery; PCA, posterior cerebral artery; VA, vertebral artery. Summary interpretation: these findings highlight a key catalytic role for hypoxaemia in cerebral OXNOS, with NO₂⁻ reduction most probably serving as the dominant vasoactive mechanism. Figure created using Biorender (<https://biorender.com/>).

Key points

- Local sampling of blood across the cerebral circulation in ultra-elite apnoeists determined the extent to which severe end-apnoea hypoxaemic hypercapnia (prior normoxic normoventilation) and hyperoxaemic hypercapnia (prior hyperoxic hyperventilation) impact free radical-mediated nitric oxide bioavailability and global cerebral bioenergetic function.
- Apnoea generally increased the net cerebral output of free radicals and suppressed plasma nitrite consumption, thereby reducing delivery of nitric oxide consistent with elevated oxidative–nitrosative stress.
- The apnoea-induced elevation in global cerebral blood flow was insufficient to prevent a reduction in the cerebral metabolic rates of oxygen and glucose.
- Cerebral oxidative–nitrosative stress was greater during hypoxaemic hypercapnia compared with hyperoxaemic hypercapnia and coincided with a lower apnoea-induced elevation in global cerebral blood flow, highlighting a key catalytic role for hypoxaemia.
- This applied model of voluntary human asphyxia might have broader implications for the management and treatment of neurological diseases characterized by extremes of oxygen demand and carbon dioxide production.

Introduction

The three gases, oxygen (O₂), carbon dioxide (CO₂) and nitric oxide (NO), in the human respiratory cycle are fundamental regulators of cerebral blood flow (CBF) that have helped to shape evolution of the mammalian brain (Bailey, 2019a, 2019c). Cerebral vasodilatation in response to hypercapnia, hypoxia and NO, with reciprocal vasoconstriction in response to hypocapnia, hyperoxia and NO inhibition, are fundamental, highly conserved integrative responses that serve to couple cerebral O₂ delivery (CDO₂) and CO₂ removal to tissue metabolic demand (Kety & Schmidt, 1948; Willie et al., 2014). This is critical, given the inherent vulnerability of the brain to hypoxia owing to its obligatory high rate of O₂ consumption in the face of limited glycolytic reserves (Scheinberg & Stead, 1949), with heightened sensitivity to

hypercapnia reflecting prioritization of acid–base balance for stabilization of chemosensory and autonomic control at the level of the brainstem (Caldwell et al., 2021; Kety & Schmidt, 1948). However, the molecular mechanisms that ‘sense’ crosstalk between these gases and coordinate transmission of adaptive signals to maintain cerebral bioenergetic homeostasis across the continuum of partial pressures remain, at best, enigmatic (Bailey et al., 2017).

Emerging evidence suggests a potentially unifying hormetic role for free radicals and associated reactive oxygen/nitrogen species (ROS/RNS) that in physiological, albeit undefined, concentrations function as adaptive signal transductants (Smith et al., 2017). Mitochondrial superoxide (O₂^{•-}) release by complex I and III of the electron transport chain (ETC) and subsequent formation of hydrogen peroxide (H₂O₂) are widely considered primary sources of ROS in

cellular hypoxia (Duranteau et al., 1998; Guzy et al., 2005), capable of triggering activation of adaptive gene expression via stabilization of hypoxia-inducible factor (HIF)- α (Chandel et al., 1998). In tandem with pH, adaptive redox signalling has also been implicated in CO₂/H⁺-mediated central chemoreception involving physiological formation of a multitude of species, notably peroxydicarbonate (HCO₄⁻) following reaction with H₂O₂ and nitrosoperoxocarbonate following reaction with peroxydicarbonate (ONOO⁻), forming carbonate radicals (CO₃⁻), nitrogen dioxide (NO₂) and nitrosoperoxocarbonate (ONO₂CO₂⁻) (Dean, 2010; Radi, 2022).

In contrast, when exaggerated and sustained, as is classically the case during hyperoxia, redox reactants transcend physiologically adaptive signalling thresholds to become pathologically maladaptive. Excessive O₂⁻ and Fenton-catalysed formation of hydroxyl (HO[•]) and lipid-derived alkoxy/alkyl (LO[•]/LC[•]) radicals can react directly with NO to yield ONOO⁻ (O₂⁻/LO[•]/LC[•] + NO $\xrightarrow{k \sim 10^9 \text{ M/s}}$ ONOO⁻) (Nauser & Koppenol, 2002), which exhibits enhanced cytotoxicity in the presence of CO₂ (Pryor et al., 2006; Radi, 2022). Furthermore, excess H⁺ formation, independent of molecular CO₂, can also trigger Fenton-induced HO[•] (Dean, 2010). Collectively, these reactions compound lipid peroxidation/protein tyrosine nitrosylation and uncouple vascular endothelial NO synthase subsequent to O₂⁻-induced tetrahydrobiopterin oxidation, further reducing intravascular NO bioavailability and potentiating endothelial dysfunction, culminating in elevated systemic/cerebral oxidative–nitrosative stress (OXNOS) (Bailey et al., 2019; Bailey, Culcasi et al., 2022). Cerebral bioenergetic function can be compromised further, given that free radicals, when unrestrained, are thermodynamically capable of initiating and propagating cellular membrane destabilization and damage, to which the brain is histologically vulnerable, given its modest antioxidant defences, abundance of transition metals, autooxidizable neurotransmitters and neuronal membrane lipids rich in eicosapentaenoic (C_{20:5}) and docosahexaenoic (C_{22:6}) polyunsaturated fatty acid side-chains exposed to an obligatory high mass-specific O₂ flux (Bailey, 2019c; Copley et al., 2018).

Although NO subserves a permissive rather than obligatory role for cerebral hypercapnic vasodilatation (Hoiland et al., 2022), systemic infusion of the nitric oxide synthase (NOS) inhibitor L-NMMA in humans indicates that up to 25% of cerebral hypoxic vasodilatation is NO dependent, with red blood cell (RBC) haemoglobin (Hb)–NO signalling a central mediator (Hoiland et al., 2023). However, despite widespread recognition that RBCs can preserve and transfer NO bioactivity ‘long distance’, the specific moieties and mechanism(s) underpinning cerebrovasoregulation across the P_{O₂}–P_{CO₂}

continuum remain widely contested, informed in part by the direction and magnitude of local arterio-jugular venous concentration differences (a–v_D) of plasma and RBC-bound NO metabolites (Bailey, Rasmussen et al., 2017; Bailey, Taudorf, Berg, Lundby et al., 2009; Hoiland et al., 2022, 2023; Premont et al., 2020).

In addition to allosterically mediated RBC release of ATP catalysed by deoxyHb-mediated purinergic (P_{2Y2} receptor) signalling (Ellsworth et al., 1995), two fundamentally different hypotheses have been proposed to elucidate hypoxic vasodilatation (Gladwin & Schechter, 2004). The first posits that Hb is an allosterically regulated haeme-based nitrite (NO₂⁻) reductase that reduces NO₂⁻ to NO or dinitrogen trioxide (N₂O₃) catalysed by deoxyHb-mediated reduction and acidic disproportionation during circulatory a–v transit (NO₂⁻ + HbFe²⁺ (deoxyHb) + H⁺ $\xrightarrow{k \sim 0.47 \text{ M/s}}$ HbFe³⁺ (metHb) + NO + OH⁻) (Bailey, Rasmussen et al., 2017; Cosby et al., 2003; Gladwin et al., 2000). The competing hypothesis contends that NO is stabilized, transported and delivered by intramolecular NO group transfers between the haeme iron and β -93 cysteine, which, upon deoxygenation, releases an as yet unidentified moiety that is exported from the RBC, involving transnitrosylation of the anion exchanger AE1, as a low-molecular-weight S-nitrosothiol (RSNO) to effect vasodilatation (Jia et al., 1996; Pawloski et al., 2001; Stamler et al., 1997). Although the debate remains unresolved, unifying, albeit emergent, evidence suggests that Hb–NO signalling is subject to redox regulation (Katona et al., 2023), although human studies that manipulate gas exchange to promote crosstalk across the ROS–RNS–NO ‘redox interactome’ are lacking.

Prolonged apnoea performed by ultra-elite breath-hold divers affords a unique experimental model to address these knowledge gaps, given its ability to evoke the most severe extremes of O₂–CO₂ stress recorded to date in conscious, otherwise healthy humans and with hypoxaemia and recovery reoxygenation being well-established redox-reactive stimuli. With breath-holds lasting >5 min, which can be extended further to >15 min after prior hyperoxic hyperventilation, apnoeists often achieve arterial partial pressures of O₂ (P_{aO₂}) of <20 mmHg, oxyHb saturation (S_{O₂}) of <40% and arterial P_{CO₂} (P_{aCO₂}) of >70 mmHg at apnoea breakpoint (Bain, Drvis et al., 2018).

In this study, we combined volumetric Doppler assessment of CBF with concurrent a–v_D sampling of OXNOS biomarkers using electron paramagnetic resonance (EPR) spectroscopy and ozone-based chemiluminescence (OBC), which are the most sensitive, specific and direct techniques for the detection and molecular identification of free radicals and nitric oxide (NO) metabolites, respectively. Our primary aim was to document transcerebral OXNOS exchange

kinetics in response to two separate maximal apnoeas specifically designed to induce end-apnoea: (i) hypoxaemic hypercapnia (apnoea preceded by normoxic normoventilation); and (ii) hyperoxaemic hypercapnia (apnoea preceded by hyperoxic hyperventilation), to tentatively disassociate hypoxaemic from hyperoxaemic hypercapnia, although we anticipated *a priori* that hypercapnia would be slightly more marked during the latter trial, given extended breath-hold times. Our secondary aim was to determine whether cerebral exchange is associated with alterations in NO bioactivity, including dominant moieties and corresponding implications for cerebral bioenergetic function, reflected by changes in global CBF (gCBF) and cerebral metabolic rates of O₂ and glucose (gCMRO₂/gCMR_{Glu}). We hypothesized that: (i) cerebral output of free radicals ($v > a$) and corresponding reduction in NO metabolite consumption ($a > v$) would be greater in hypoxaemic compared with hyperoxaemic hypercapnia, suppressing apnoea-induced elevations in gCBF, gCMRO₂ and gCMR_{Glu}, implicating hypoxaemic hypercapnia as the dominant cerebral OXNOS catalyst (Fig. 1A); and (ii) apnoea-induced elevations in gCBF, gCMRO₂ and gCMR_{Glu} would be associated generally with a combined uptake ($a > v$) of the vasoactive moieties NO₂⁻, RSNO and SNO-Hb, collectively taken to reflect metabolite consumption and local delivery of bioactive NO, to support cerebral bioenergetic demand.

Methods

Ethical approval

Experimental procedures were approved by the University of Split, Ethics Committee (#H14-00922). All procedures were carried out in accordance with the most recent (seventh) amendment of the *Declaration of Helsinki* of the World Medical Association (WMA, 2013) (with the exception that it was not registered in a publicly accessible database prior to recruitment), with verbal and written informed consent obtained from all participants.

Participants

Ten physically active, ultra-elite apnoeists (six men and four women) aged 33 (mean) ± 9 (SD) years old, with a body mass index of 23 ± 2 kg/m² and forced vital capacity of 6.40 ± 1.48 L, volunteered from the Croatian National Apnoea Team. At the time of these experiments, six had placed within the world's top 10 within the last 5 years. One woman set a new official world record in dynamic apnoea and a man set the world record for apnoea following prior hyperoxic hyperventilation (24 min 33 s). A medical examination confirmed that all participants were free of cardiovascular, pulmonary

and cerebrovascular disease and were not taking any nutritional supplements, including over-the-counter antioxidant or anti-inflammatory medications. They were advised to refrain from physical activity, caffeine and alcohol for 24 h before formal experimentation. Participants were also encouraged to maintain their normal dietary behaviour, with the exception of avoiding foods rich in nitrates/nitrites, specifically fruits, salads and cured meats (Wang et al., 1997), although we did not perform any formal dietary analyses to confirm compliance with our requests.

Design

Parts of this study including blood gas and select aspects of metabolic and cerebral haemodynamic function (Tables 1 and 2 and Fig. 2) have previously been published as part of separate complementary investigations focused on the link between hypercapnia and cerebral oxidative metabolism (Bain et al., 2017) and hyperperfusion-mediated structural destabilization of the neurovascular unit (Bailey, Bain et al., 2022). Thus, although the present study adopted an identical experimental design (non-randomized cross-over repeated measures trial), it constitutes an entirely separate investigation complemented by *de novo* experimental measures and *a priori* hypotheses focused exclusively on altered redox homeostasis. Participants were required to perform two maximal apnoeas preceded by: (i) normoxic normoventilation resulting in severe (end-apnoea) hypoxaemic hypercapnia; and (ii) hyperoxic hyperventilation designed to prevent hypoxaemia, resulting in hyperoxaemic hypercapnia. The order of trials was non-randomized, given the long-lasting carryover effects of hyperoxia and fatigue associated with a more prolonged apnoea (Bain et al., 2017). Data were collected at eupnoea baseline and timed to coincide with the point of apnoea termination, with a 30 min inter-trial recovery to ensure full participant recovery (Bain et al., 2017).

Procedures

All apnoeas were completed on a single day, with the Croatian national apnoea coach present to motivate divers and ensure maximal efforts. Each apnoea was preceded by 30 min of supine rest followed by two standardized preparatory (practice) apnoeas designed to maximize the experimental apnoeas (see below). The first preparatory apnoea was performed at functional residual capacity until seven involuntary breathing movements (IBMs) were attained. Two minutes later, the second preparatory apnoea was performed at total lung capacity lasting for 10 IBMs. Participants then rested quietly for 6 min prior to two 'maximal' apnoeas that were each performed at total lung capacity.

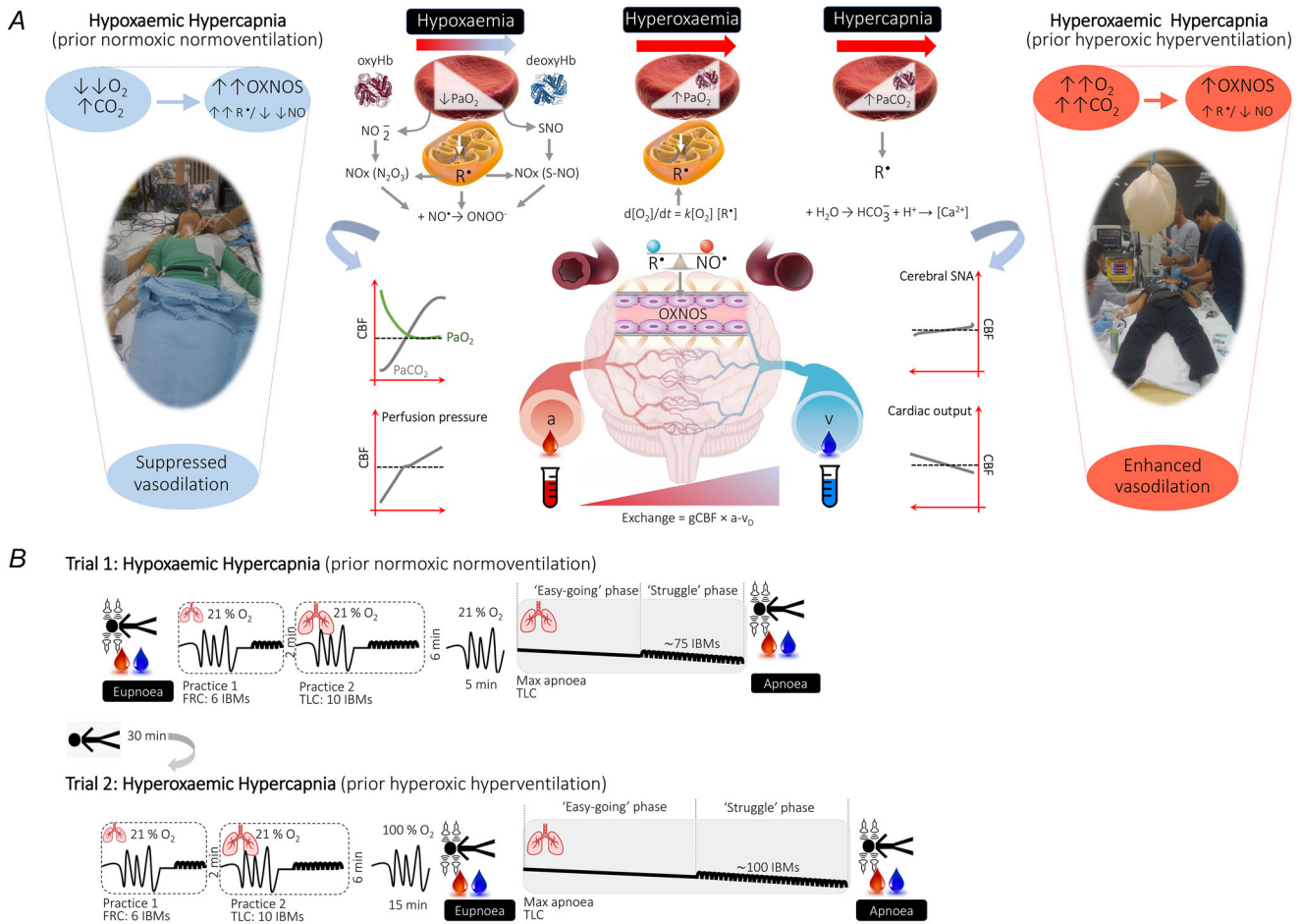


Figure 1. Experimental hypotheses (A) and design (B)

A, predicted differential disruption of cerebral redox homeostasis and implications for cerebral bioenergetic function in response to pathological extremes of oxygen (O_2) demand and carbon dioxide (CO_2) production invoked by (end-apnoea) hypoxaemic hypercapnia (prior normoxic normoventilation) and hyperoxaemic hypercapnia (prior hyperoxic hyperventilation) apnoeas. The O_2/CO_2 sensing by the red blood cell (RBC) and mitochondrion is allosterically coupled to formation of nitric oxide (NO^*) (Huang et al., 2005) and reactive oxygen/nitrogen (ROS/RNS) (Guzy et al., 2005) species that titrate (global) cerebral blood flow (gCBF), coupling substrate (O_2 and glucose) delivery to demand. The more marked reduction in arterial partial pressure of oxygen (P_{aO_2}) during the hypoxaemic hypercapnia trial is hypothesized to induce a greater elevation in cerebral oxidative–nitrosative stress (OXNOS), reflected by a free radical-mediated reduction in vascular NO bioavailability manifest as increased net cerebral output (venous > arterial) of free radicals and lipid peroxidants and corresponding lower net cerebral uptake (arterial > venous) of nitrite (NO_2^-) or S-nitrosohaemoglobin (SNO-Hb), leading to a suppression of cerebral hypoxic vasodilatation relative to the hyperoxaemic hypercapnia trial. Note the typical human experimental set-up, highlighting arterial–jugular venous (transcerebral) sampling of blood combined with volumetric assessment of gCBF. Abbreviations: a–vD, arterio–jugular venous concentration difference; NO_2^- , nitrite; N_2O_3 , nitrogen tri-oxide; $ONOO^-$, peroxynitrite (not measured); P_{aCO_2} , arterial partial pressure of carbon dioxide; P_{aO_2} , arterial partial pressure of oxygen; R^* , free radical; SNA, sympathetic nervous activity (not measured). B, two submaximal (practice) apnoeas preceded separate trials involving (i) prior normoxic (21% O_2) normoventilation, resulting in severe hypoxaemic hypercapnia apnoea, and (ii) prior hyperoxic hyperventilation (100% O_2), designed to ablate hypoxaemia, resulting in hyperoxaemic hypercapnia. The first practice apnoea was performed at functional residual capacity (FRC) for six involuntary body movements (IBMs) and the second practice at total lung capacity (TLC) for 10 IBMs. Both maximal apnoeas were performed at TLC. Measurements were performed at eupnoea baseline and timed to coincide with the end of each maximal apnoea. Figure created using Biorender (<https://biorender.com/>).

Table 1. Blood gas variables	Hypoxaemic hypercapnia (n = 10)						Hyperoxaemic hypercapnia (n = 10)					
	Eupnoea			Apnoea			Eupnoea			Apnoea		
	Arterial	Venous		Arterial	Venous		Arterial	Venous		Arterial	Venous	
Trial:	Hypoxaemic hypercapnia (n = 10)						Hyperoxaemic hypercapnia (n = 10)					
State:	Eupnoea			Apnoea			Eupnoea			Apnoea		
Site:	Arterial	Venous		Arterial	Venous		Arterial	Venous		Arterial	Venous	
P_{O₂} (mmHg)	97 ± 12	34 ± 4		36 ± 5*	28 ± 5*		589 ± 23 [†]	28 ± 10		425 ± 79* [†]	80 ± 9* [†]	
	Trial (P < 0.001); State (P < 0.001); Site (P < 0.001); Trial × State (P < 0.001); State × Site (P < 0.001); Trial × State × Site (P = 0.008)											
S_{O₂} (%)	98 ± 1	58 ± 7		60 ± 11*	40 ± 11*		100 ± 0 [†]	51 ± 19		100 ± 0 [†]	93 ± 2* [†]	
	Trial (P < 0.001); State (P < 0.001); Trial × State (P < 0.001); State × Site (P < 0.001); Trial × State × Site (P = 0.006)											
CO₂ (ml/dl)	18.3 ± 1.7	10.7 ± 1.6		11.7 ± 2.4*	8.0 ± 2.6*		20.6 ± 2.0 [†]	9.7 ± 3.6		20.0 ± 1.6* [†]	17.8 ± 1.9* [†]	
	Trial (P < 0.001); State (P < 0.001); Trial × State (P < 0.001); State × Site (P < 0.001); Trial × State × Site (P = 0.006)											
P_{CO₂} (mmHg)	36 ± 5	47 ± 5		51 ± 3*	54 ± 4*		16 ± 4 [†]	31 ± 6 [†]		58 ± 5* [†]	59 ± 15*	
	Trial (P < 0.001); State (P < 0.001); Trial × State (P < 0.001); State × Site (P < 0.001); Trial × State × Site (P = 0.033)											
pH (units)	7.440 ± 0.043	7.384 ± 0.032		7.360 ± 0.023*	7.348 ± 0.021*		7.700 ± 0.078 [†]	7.542 ± 0.071 [†]		7.283 ± 0.043* [†]	7.306 ± 0.154*	
	Trial (P = 0.005); State (P < 0.001); Site (P = 0.001); Trial × State (P < 0.001); State × Site (P < 0.001); Trial × State × Site (P = 0.008)											
H⁺ (μM)	36 ± 3	41 ± 3		44 ± 2	45 ± 2		20 ± 4	29 ± 4		52 ± 5	52 ± 12	
	Trial (P < 0.001); State (P = 0.001); Site (P = 0.001); Trial × State (P < 0.001); State × Site (P < 0.001); Trial × State × Site (P < 0.001)											
HCO₃⁻ (mM)	24.2 ± 2.5	27.9 ± 2.3		27.9 ± 3.1*	29.8 ± 2.0*		19.8 ± 2.0 [†]	26.0 ± 2.2 [†]		27.2 ± 1.9*	27.9 ± 2.1* [†]	
	Trial (P = 0.001); State (P < 0.001); Site (P < 0.001); Trial × State (P = 0.002); State × Site (P < 0.001); Trial × State × Site (P < 0.001)											
Hb (g/dl)	13.7 ± 1.4	13.7 ± 1.4		14.3 ± 1.2	14.5 ± 1.0		14.0 ± 1.4	14.2 ± 1.5		14.0 ± 1.2	14.1 ± 1.4	
	Trial × State (P = 0.034)											
Hct (%)	42 ± 4	42 ± 4		44 ± 4	44 ± 3		43 ± 4	44 ± 5		43 ± 4	43 ± 4	
	Trial × State (P = 0.023)											

Values are mean ± SD based on 10 participants. *Different between State for given Trial and Site (P < 0.05); [†]different between Trial for given State and Site (P < 0.05). Data were analyzed using three-factor (Trial: hypoxaemic hypercapnia vs. hyperoxaemic hypercapnia × State: eupnoea vs. apnoea × Site: arterial vs. venous) repeated-measures ANOVA. Post hoc Bonferroni-corrected Student's paired samples t tests were used to locate differences following an interaction. Summary interpretation: the hypoxaemic hypercapnia trial induced severe hypoxaemia, hypercapnia and metabolic acidosis, whereas participants were, by design, more hypercapnic at baseline eupnoea owing to prior hyperoxic hyperventilation where they remained hyperoxaemic and even more hypercapnic/acidotic at end-apnoea in the hyperoxaemic hypercapnia trial. Abbreviations: P_{O₂}/P_{CO₂}, partial pressure of oxygen/carbon dioxide; S_{O₂}, oxyhaemoglobin saturation; CO₂, oxygen content; Hb, haemoglobin; Hct, haematocrit.

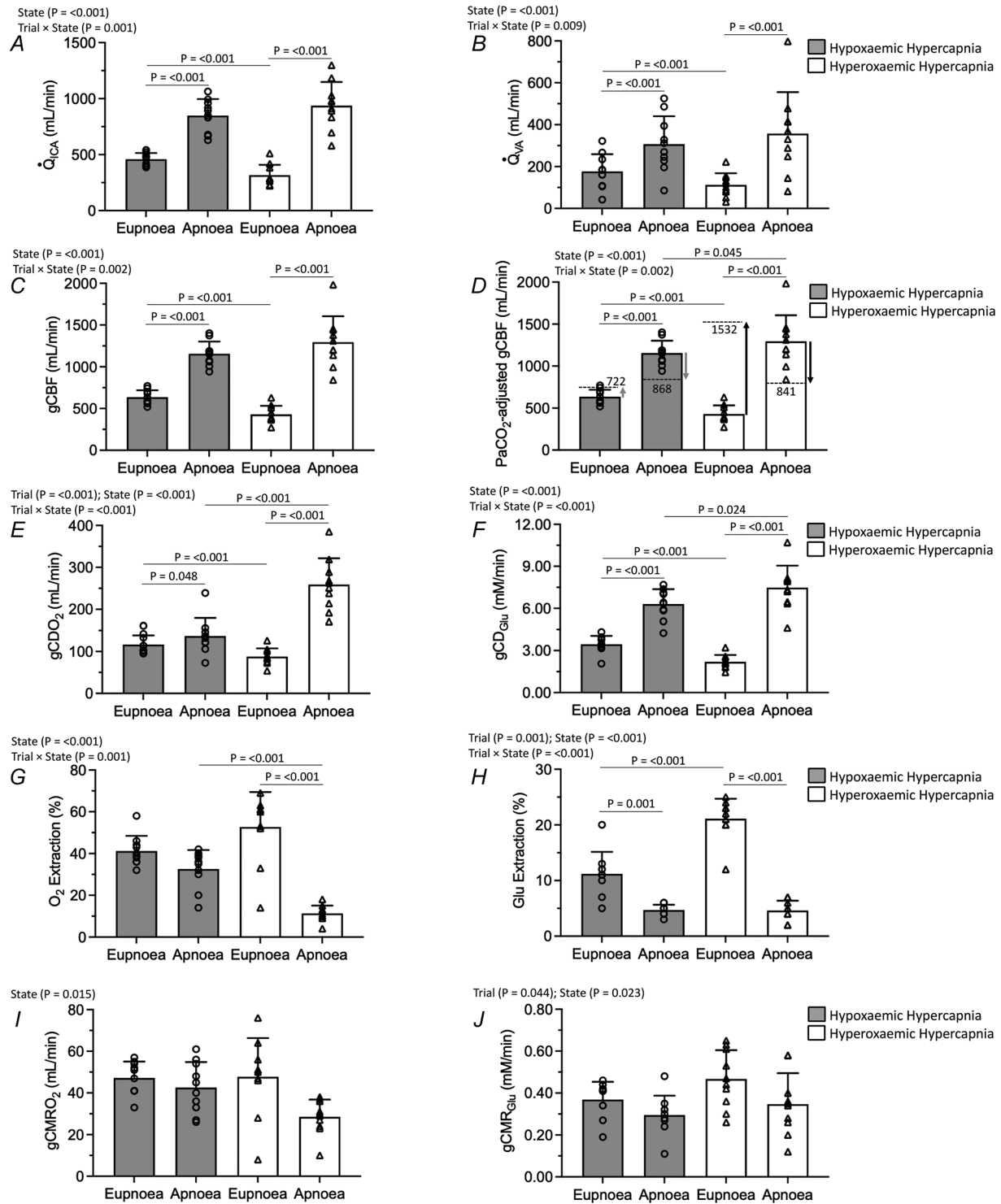


Figure 2. Cerebral bioenergetic function

Values are mean \pm SD based on 10 participants. Circles and triangles denote individual data points for participants during the hypoxaemic hypercapnia and hyperoxaemic hypercapnia trials, respectively. Abbreviations: CMR, cerebral metabolic rate; gCBF, global cerebral blood flow; gCD_{Glu}, global cerebral delivery of glucose; gCDO₂, global cerebral delivery of oxygen; \dot{Q}_{ICA} , internal carotid artery flow; \dot{Q}_{VA} , vertebral artery flow. The arterial partial pressure of carbon dioxide (P_{aCO_2})-adjusted gCBF highlights theoretical (i.e. expected) values (differences highlighted by stippled lines/arrows and absolute gCBF values annotated) calculated following normalization for prevailing hypo/hypercapnia assuming a 'fixed' normocapnic P_{aCO_2} of 40 mmHg and 1 mmHg bidirectional change in P_{aCO_2} equates to 3% bidirectional change in gCBF (see Methods). Data were analyzed using two-factor (Trial:

hypoxaemic hypercapnia vs. hyperoxaemic hypercapnia × State: eupnoea vs. apnoea) repeated-measures ANOVA. *Post hoc* Bonferroni-corrected Student's paired samples *t* tests were used to locate differences following an interaction. Summary interpretation: the apnoea-induced (relative) increase in cerebral perfusion and consequent substrate delivery were selectively blunted in the hypoxaemic hypercapnia trial. Reciprocal reductions in substrate extraction translated into apnoea-induced reductions in cerebral metabolism, which, for glucose, was generally lower in the hypoxaemic hypercapnia trial.

Trial 1: prior normoxic normoventilation (hypoxaemic hypercapnia apnoea). Participants performed a maximal apnoea in room air (normoxia).

Trial 2: prior hyperoxic hyperventilation (hyperoxaemic hypercapnia apnoea). Participants performed a maximal apnoea preceded by 15 min of hyperventilation of 100% O₂ while receiving auditory feedback from the coach to achieve an end-tidal partial pressure of carbon dioxide (P_{ET,CO_2}) of ~20 mmHg.

Blood sampling

Catheterization. Participants were placed slightly head down on a hospital bed, and two catheters were inserted retrograde using the Seldinger technique under local anaesthesia (1% lidocaine) via ultrasound guidance. A 20-gauge arterial catheter (Arrow, Markham, ON, Canada) was placed in the right radial artery and attached to an in-line wasteless sampling set-up (Edwards Life-

sciences VAMP, CA, USA) connected to a pressure transducer that was placed at the height of the right atrium (TruWave transducer). A central venous catheter (Edwards PediaSat Oximetry Catheter, CA, USA) was placed in the right internal jugular vein and advanced towards the jugular bulb located at the mastoid process, approximately at the C1–C2 interspace (Fig. 1). Facial vein contamination was ruled out by ensuring that all jugular venous oxyhaemoglobin saturation (SO₂) values were <75% at rest. Participants rested for ≥30 min following catheter placement before the collection of baseline samples.

Collection and storage. Blood samples were drawn without stasis simultaneously from the radial artery and jugular vein directly into Vacutainers (Becton, Dickinson and Company, Oxford, UK) before centrifugation at 600g (4°C) for 10 min. With the exception of blood for determination of blood gas variables, plasma and RBC samples were decanted into cryogenic vials (Nalgene

Table 2. Cardiopulmonary function

Trial:	Hypoxaemic hypercapnia (n = 10)			Hyperoxaemic hypercapnia (n = 10)		
	Eupnoea	Apnoea	Δ	Eupnoea	Apnoea	Δ
HR (beats/min)	64 ± 7	59 ± 14	-5 ± 12	65 ± 11	69 ± 13	4 ± 18
SV (ml/min)	78 ± 16	67 ± 16*	-11 ± 15	86 ± 17†	90 ± 17†	5 ± 12†
Trial (P = 0.001); Trial × State (P = 0.001)						
Q̇ (L/min)	4.92 ± 0.91	3.91 ± 1.17*	-1.01 ± 1.21	5.46 ± 1.01	6.29 ± 1.97†	0.83 ± 1.73†
Trial (P = 0.001); Trial × State (P = 0.029)						
MAP (mmHg)	116 ± 8	177 ± 8*	61 ± 9	111 ± 8†	158 ± 16*†	47 ± 14*†
Trial (P = 0.001); State (P < 0.001); Trial × State (P = 0.018)						
TPR (mmHg/L/min)	24 ± 5	50 ± 18*	25 ± 18	21 ± 4†	27 ± 10*†	7 ± 9†
Trial (P < 0.001); State (P < 0.001); Trial × State (P = 0.012)						
IJVP (mmHg)	10 ± 2	22 ± 1*	12 ± 2	10 ± 2	17 ± 5*†	7 ± 5*†
Trial (P = 0.015); State (P < 0.001); Trial × State (P = 0.016)						
CPP (mmHg)	106 ± 9	155 ± 7	49 ± 8	101 ± 9	141 ± 16	40 ± 13
Trial (P = 0.002); State (P < 0.001); Trial × State (P = 0.112)						

Values are the mean ± SD based on 10 participants. Data were analyzed using two-factor (Trial: hypoxaemic hypercapnia vs. hyperoxaemic hypercapnia × State: eupnoea vs. apnoea) repeated-measures ANOVA. *Post hoc* Bonferroni-corrected Student's paired samples *t* tests were used to locate differences following an interaction. *Different between State for given Trial (P < 0.05); †different between Trial for given State or Δ (P < 0.05). Summary interpretation: with the exception of an apnoea-induced reduction in Q̇, elevations in MAP, TPR, IJVP and CPP were collectively greater in the hypoxaemic hypercapnia trial. Abbreviations: CPP, cerebral perfusion pressure; Δ, apnoea minus eupnoea; HR, heart rate; IJVP, internal jugular venous pressure; MAP, mean arterial pressure; Q̇, cardiac output; SV, stroke volume; TPR, total peripheral resistance.

Labware, Thermo Fisher Scientific, Waltham, MA, USA) and immediately snap-frozen in liquid nitrogen (N₂) before transport under nitrogen gas (Cryopak, Taylor-Wharton, Theodore, AL, USA) from Croatia to the UK. Samples were left to defrost at 37°C in the dark for 5 min before batch analysis.

Measurements

Blood gases. Whole blood was collected into heparinized syringes, maintained anaerobically at room temperature and immediately analyzed for Hb, haematocrit (Hct), P_{O_2} , P_{CO_2} , S_{O_2} , pH and glucose (Glu) using a commercially available cassette-based analyzer (ABL-90 FLEX, Radiometer, Copenhagen, Denmark). Hydrogen ion (H⁺) concentration was calculated as $[H^+] = 10^{-pH}$. The intra- and inter-assay coefficients of variation (CVs) for all metabolites were both <5% (Bailey et al., 2018).

Antioxidants. Plasma was stabilized and deproteinated using 10% metaphosphoric acid (Sigma Chemical, UK). Ascorbic acid was assayed by fluorimetry, based on the condensation of dehydroascorbic acid with 1,2-phenylenediamine (Vuilleumier & Keck, 1993). The total concentration of the lipid soluble antioxidants (LSA), encompassing individually measured concentrations of α/γ -tocopherol, α/β -carotene, retinol and lycopene, was determined using high-performance liquid chromatography (Catignani & Bieri, 1983; Thurnham et al., 1988). The intra- and inter-assay CVs for all metabolites were both <5% (Bailey et al., 2018).

Free radicals

Ascorbate free radical. We used EPR spectroscopic detection of ascorbate free radical (A^{•-}) as a direct measure of global systemic free radical formation (Bailey et al., 2018). Plasma (1 ml) was injected directly into a high-sensitivity multiple-bore sample cell (AquaX, Bruker Daltonics Inc., Billerica, MA, USA) housed within a TM₁₁₀ cavity of an EPR spectrometer operating at X-band frequency (9.87 GHz). Samples were recorded by cumulative signal averaging of 10 scans using the following instrument parameters: resolution, 1024 points; microwave power, 20 mW; modulation amplitude, 0.65 G; receiver gain, 2×10^6 ; time constant, 40.96 ms; sweep rate, 0.14 G/s; sweep width, 6 G; and centre field, 3486 G. All spectra were filtered identically (moving average, 15 conversion points) using WINEPR software (v.2.11; Bruker, Karlsruhe, Germany) and the double integral of each doublet quantified using Origin 8 software (OriginLab Corps, MA, USA). The intra- and inter-assay CVs were both <5% (Bailey et al., 2018).

Lipid hydroperoxides. Lipid hydroperoxides (LOOH) were determined spectrophotometrically via the ferric oxidation of xylenol orange (FOX) version II method, with modification (Bailey et al., 2018). Intra- and inter-assay CVs were <2% and <4%, respectively (Bailey et al., 2018).

Nitric oxide metabolites. The modified triiodide-based chemiluminescence assay (Sievers NOA 280i, Analytix, Durham, UK), which includes addition of potassium ferricyanide to prevent NO autocapture by deoxygenated Hb/cell-free haem, was used to detect plasma and RBC-bound NO₂⁻, S-nitrosothiols (RSNO), S-nitrosohaemoglobin (SNO-Hb) and iron nitrosylhaemoglobin (HbNO) (Bailey, Rasmussen et al., 2017; Pinder et al., 2009; Rogers et al., 2005). Total NO bioactivity was calculated as the cumulative concentration of all individual, potentially bioactive plasma and RBC metabolites, to assist with general interpretation similar to total LSA (intra- and inter-assay CVs were 7% and 8%, respectively). Signal output was plotted against time using Origin 8 software (OriginLab Corps) and smoothed using a 150-point averaging algorithm. The Peak Analysis package was used to calculate the area under the curve and subsequently converted to a concentration using standard curves of sodium NO₂⁻. Intra- and inter-assay CVs for all metabolites were both <10% (Bailey, Rasmussen et al., 2017).

Cardiopulmonary function. All cardiopulmonary measurements were averaged over 15 s immediately before blood sampling. A lead II electrocardiogram (Dual BioAmp; ADInstruments, Oxford, UK) was used to measure heart rate (HR). Intra-arterial ABP was recorded directly via a pressure transducer placed at the level of the heart for determination of mean arterial pressure (MAP). Internal jugular venous pressure (IJVP) was measured with the transducer connected to the jugular catheter. The end-tidal partial pressure of oxygen (P_{ET,O_2}) and P_{ET,CO_2} were measured via capnography (ML 206, ADInstruments, Oxford, UK). Finger photoplethysmography (Finometer PRO, Finapres Medical Systems, Amsterdam, The Netherlands) was used to measure beat-by-beat stroke volume (SV) and cardiac output (\dot{Q}) using the Modelflow algorithm (Wesseling et al., 1993), which incorporates participant sex, age, stature and mass (BeatScope 1.0 software; TNO; TPD Biomedical Instrumentation, Amsterdam, The Netherlands). Total peripheral resistance (TPR) was calculated as MAP/\dot{Q} .

Cerebrovascular function

Intracranial. Contralateral continuous assessments of blood velocity in the middle cerebral artery (MCAv; insonated through the left temporal window) and post-

erior cerebral artery (PCAv; insonated at the P1 segment through the right temporal window) were measured using standardized procedures with a 2 MHz pulsed transcranial Doppler ultrasound (TCD; Spencer Technologies, Seattle, WA, USA). Bilateral TCD probes were secured using a specialized commercial headband (Mark600, Spencer Technologies, Seattle, WA, USA) using standardized search techniques.

Extracranial. Contralateral continuous assessments of diameter, velocity and blood flow recordings in the right internal carotid and left vertebral arteries ($\dot{Q}_{ICA}/\dot{Q}_{VA}$) were obtained using a 10 MHz, multifrequency, linear array vascular ultrasound (Terason 3200, Teratech, Burlington, MA). Arterial diameter was measured via B-mode imaging, whereas peak blood velocity was measured simultaneously with pulse-wave mode. The ICA was insonated ≥ 1.5 cm from the carotid bifurcation, with no evidence of turbulent or retrograde flow present during recording. The VA was insonated at the C4–C5 or C5–C6 vertebral segment and standardized within participants for both trials. The steering angle was fixed to 60°, and the sample volume was placed in the centre of the vessel and adjusted to cover the entire vascular lumen. All images were recorded as video files at 30 Hz and stored for offline analysis using customized edge-detection software designed to mitigate observer bias (Woodman et al., 2001). Simultaneous measures of arterial diameter and velocity over >12 consecutive cardiac cycles were used to calculate flow. Between-day CVs for \dot{Q}_{ICA} and \dot{Q}_{VA} are 5% and 11%, respectively (Willie et al., 2012).

Data integration

All cardiopulmonary measurements were sampled at 1 kHz, integrated into PowerLab and LabChart software (ADInstruments, Bella Vista, NSW, Australia) for online monitoring and saved for offline analysis.

Calculations

Cerebral bioenergetics. *Perfusion:* Volumetric blood flow was calculated offline as:

$$\dot{Q}_{ICA} \text{ (ml/min)} = \frac{\text{peak envelope blood velocity}}{2} \times [\pi(0.5 \times \text{diameter})^2] \times 60 \text{ (and same for } \dot{Q}_{VA}\text{)}.$$

Values of \dot{Q}_{ICA} and \dot{Q}_{VA} were averaged for a 1 min eupnoea baseline and during the last 30 s of apnoea.

During the final $\sim 20\%$ of each respective apnoea, IBMs and corresponding contractions of the diaphragm and sternocleidomastoid precluded reliable recordings of blood velocity traces, whereas we were still able to track ICA and VA diameter reliably up to breath-hold

termination for volumetric flow calculations. To circumvent this, \dot{Q}_{ICA} and \dot{Q}_{VA} were estimated from (percentage) changes in MCAv (for \dot{Q}_{ICA}) and PCAv (for \dot{Q}_{VA}), respectively, as previously described (Hoiland, Ainslie et al., 2017; Willie et al., 2015):

$$\begin{aligned} & \text{Estimated apnoea ICAv and VAv (percentage changes)} \\ &= \text{Pre} - \text{IBM ICAv and VAv} \\ & \times \left(\frac{\text{Apnoea MCAv and PCAv}}{\text{Pre} - \text{IBM MCAv and PCAv}} \right) \times 100 \end{aligned}$$

The term ‘Pre-IBM ICAv and VAv’ represents the average velocity of the last 30 s before the IBMs when reliable velocity traces were no longer attainable. The latter part of the equation (percentage change in MCAv and PCAv) represents the relative increases in MCAv and PCAv from the same pre-IBM stage. Volumetric extracranial flow was subsequently calculated from the estimated (e) velocity values and measured vessel cross-sectional area, with the latter ensuring that flow was not underestimated using indirect metrics of MCAv and PCAv only (Coverdale et al., 2014):

$$\begin{aligned} & \dot{Q}_{ICA} \text{ and } \dot{Q}_{VA} \text{ (ml/min)} \\ &= e\text{ICA}v \text{ or } e\text{VA}v \times \pi \left(\frac{\text{diameter}}{2} \right)^2 \end{aligned}$$

Assuming symmetrical blood flow of contralateral ICA and VA (see ‘*Experimental limitations*’ in the Discussion), global cerebral blood flow (gCBF) was calculated as:

$$\text{gCBF (ml/min)} = 2 \times (\dot{Q}_{ICA} + \dot{Q}_{VA})$$

Prior research conducted by our group applied Pearson product–moment correlations between percentage changes in ICAv and VAv with those of MCAv and PCAv, respectively, recorded ‘continuously’ over the course of $\geq 50\%$ of the apnoea (i.e. until velocity measures became unattainable owing to excessive IBMs), with continuous assessment of vessel luminal diameter. The latter inclusion ensured that gCBF was not underestimated using indirect (MCAv and PCAv) metrics only (Coverdale et al., 2014). The (average) within-subject r^2 values for the relationship(s) between ICAv and MCAv ranged from 0.70–0.90 and 0.70–0.95 for VAv and PCAv (Bain et al., 2016; Hoiland, Ainslie et al., 2017), highlighting excellent agreement between confluent intra- and extracranial blood velocities, thus supporting current derivations of gCBF at end-apnoea. Furthermore, we have previously demonstrated that MCAv and ICAv reactivity do not differ statistically over a wide range of end-tidal P_{CO_2} values (from normocapnea baseline to +9 mmHg) (Hoiland et al., 2016). Equally, ICAv and VAv reactivity have previously been shown to be comparable to MCAv and PCAv reactivity, respectively, during hypoxia across a

continuum of arterial oxyhaemoglobin saturation (S_{aO_2}) values (98, 90, 80 and 70%) (Hoiland, Bain et al., 2017).

We also chose to 'adjust' gCBF to determine 'expected' values independently of changes in P_{aCO_2} in an attempt to define better the theoretical perfusion changes attributable to prevailing hypoxaemia or hyperoxaemia *per se*. To do this, gCBF was corrected according to a theoretical 'fixed' normocapnic P_{aCO_2} of 40 mmHg and assuming 1 mmHg bidirectional change in P_{aCO_2} equates to 3% bidirectional change in gCBF using the following equation:

$$\text{Adjusted gCBF (ml/min)} = \frac{\text{measured gCBF (mL/min)}}{[1 + [\text{measured PaCO}_2 \text{ (mmHg)} - \text{normocapnic PaCO}_2 \text{ (40 mmHg)}] \times 0.03}$$

(Bailey, Taudorf, Berg, Jensen et al., 2009).

Cerebral perfusion pressure (CPP) was calculated as MAP – IJVP, with the latter serving as a surrogate for ICP (Myerson & Loman, 1932).

Metabolism: Arterial and jugular venous oxygen content (C_{aO_2} and C_{vO_2} , respectively) were calculated as:

$$C_{aO_2} \text{ (ml/dl)} = \text{Hb (g/dl)} \times 1.34 \left(\frac{S_{aO_2} (\%)}{100} \right) + 0.003 \times P_{aO_2}$$

$$C_{vO_2} \text{ (ml/dl)} = \text{Hb (g/dl)} \times 1.34 \left(\frac{S_{vO_2} (\%)}{100} \right) + 0.003 \times P_{vO_2}$$

where 1.34 is the O_2 binding capacity of Hb and 0.003 is the solubility of O_2 dissolved in blood.

Global cerebral O_2 delivery (gCDO₂) and global cerebral glucose delivery (gCD_{Glu}) were calculated as:

$$\text{gCDO}_2 \text{ (ml/min)} = \left(\frac{\text{gCBF (ml/min)}}{100} \right) \times C_{aO_2} \text{ (ml/dl)}$$

$$\text{gCD}_{\text{Glu}} \text{ (mmol/min)} = \left(\frac{\text{gCBF (ml/min)}}{1000} \right) \times a_{\text{Glucose}} \text{ (mmol/L)}$$

Oxygen and glucose extraction were calculated as:

$$O_2 \text{ extraction (\%)} = \left(\frac{C_{aO_2} \text{ (ml/dl)} - C_{vO_2} \text{ (ml/dl)}}{C_{aO_2} \text{ (ml/dl)}} \right) \times 100$$

$$\text{Glucose extraction (\%)} = \left(\frac{a_{\text{Glu}} \text{ (mM)} - v_{\text{Glu}} \text{ (mM)}}{a_{\text{Glu}} \text{ (mM)}} \right) \times 100$$

The cerebral metabolic rate of oxygen (CMRO₂) and glucose (CMR_{Glu}) were calculated as:

$$\text{CMRO}_2 \text{ (mL/min)} = \left(\frac{\text{gCBF (ml/min)}}{100} \right) \times C_{aO_2} - C_{vO_2} \text{ (ml/dl)}$$

$$\text{CMR}_{\text{Glu}} \text{ (mmol/min)} = \left(\frac{\text{gCBF (ml/min)}}{1000} \right) \times a_{\text{Glu}} - v_{\text{Glu}} \text{ (mmol/L)}$$

Transcerebral exchange kinetics. The gCBF was converted into global cerebral plasma (gCPF) and red blood cell (gCRBCF) flow:

$$\text{gCPF (ml/min)} = \text{gCBF} \left(1 - \frac{\text{Hcta}}{100} \right)$$

$$\text{gCRBCF (ml/min)} = \text{gCBF} \left(\frac{\text{Hcta}}{100} \right)$$

for corresponding calculation of net transcerebral exchange kinetics of plasma/serum/RBC-borne metabolites according to the Fick principle:

$$\text{Exchange (\mu mol or nmol/min)} = \text{gCBF} [\text{non} - (P_{aCO_2}) - \text{adjusted value}] \text{ or gCPF or gCRBCF} \times (a - v_D).$$

By convention, a positive value ($a > v$) refers to net cerebral uptake (loss or consumption), whereas a negative value ($v > a$) indicates net cerebral output (gain or formation) across the cerebrovascular bed.

Data analysis

Power calculations and sample size estimates.

Prospective power calculations and sample size estimates were performed using G*Power 3.1 software. Assuming comparable differences and corresponding effect sizes in the transcerebral exchange of plasma A^+ ($\eta^2 = -1.132$), NO_2^- ($\eta^2 = -1.000$) and RSNO ($\eta^2 = 1.444$) and gCBF ($\eta^2 = 2.020$) previously observed in a comparable group of ultra-elite apnoeists performing hypoxaemic hypercapnic apnoea (Bain, Ainslie et al., 2018), the present study required a (minimum) sample size of 9, 10, 6 and 5 participants, respectively, to achieve a power ($1 - \beta$) of 0.80 at $P < 0.05$. The repeated-measures design in the present study would have increased power further. We chose to recruit 10 participants given the potential for incomplete data collection.

Inferential statistics. Data were analyzed using the Statistics Package for Social Scientists (IBM SPSS Statistics v.29.0). Distribution normality was confirmed using Shapiro–Wilk W tests ($P > 0.05$). Data were analyzed using a combination of two-factor (State: eupnoea vs. apnoea × Site: arterial vs. venous) and three-factor (Trial: hypoxaemic hypercapnia vs. hyperoxaemic hypercapnia × State: eupnoea vs. apnoea ×

Site: arterial *vs.* venous) repeated measures ANOVA. *Post hoc* Bonferroni-corrected Student's paired samples *t* tests were used to locate differences following an interaction. Biological sex differences were (retrospectively) assessed using Mann–Whitney *U* tests, given that data were not normally distributed (Shapiro–Wilk *W* test *P*-values < 0.05). Relationships between selected variables were analyzed using Pearson product–moment correlations. Significance was established at *P* < 0.05 for all two-tailed tests, and data are presented as mean ± SD.

Results

Apnoea

Breath-hold times increased from 306 ± 62 s (range, 217–409 s) in the hypoxaemic hypercapnia trial to 959 ± 201 s (range, 579–1262 s) in the hyperoxaemic hypercapnia trial (*P* < 0.001).

Blood gas variables

As anticipated, the hypoxaemic hypercapnia trial induced severe systemic and local hypoxaemia (↓*P*_{O₂}, ↓*S*_{O₂} and ↓*C*_{O₂}), hypercapnia (↑*P*_{CO₂}) and metabolic acidosis (↓pH and ↑HCO₃⁻) at end-apnoea (all main/interaction effects, *P* = 0.033 to <0.001; Table 1). In one participant, nadirs of 29 mmHg and 40% were recorded for *P*_{aO₂} and *S*_{aO₂}, respectively, corresponding to a (peak) *P*_{aCO₂} of 53 mmHg. Venous O₂ saturation did not fall further, possibly owing to a pulmonary diffusion capacity limitation subsequent to reduced capillary transit time mediated by an elevated \dot{Q} . During the hyperoxaemic hypercapnia trial, participants were more hypocapnic at baseline eupnoea (*P*_{aCO₂}, 16 ± 4 *vs.* 36 ± 5 mmHg, *P* < 0.001) and remained hyperoxaemic and comparatively less hypertensive (MAP, 158 ± 16 *vs.* 177 ± 8 mmHg, *P* = 0.002) and more hypercapnic (*P*_{aCO₂}, 58 ± 5 *vs.* 51 ± 3 mmHg, *P* = 0.010) and acidotic (arterial pH, 7.283 ± 0.043 *vs.* 7.360 ± 0.023 units, *P* < 0.001) at end-apnoea (Table 1). The highest individual value recorded for *P*_{aCO₂} at end-apnoea was 68 mmHg, corresponding to a pH of 7.227. Baseline Hb and Hct at eupnoea were also elevated in the hyperoxaemic hypercapnia trial (Trial × State, *P* = 0.034; Table 1).

Cardiopulmonary function

Selective decreases in SV (*P* = 0.039) and \dot{Q} (*P* = 0.027) were observed in the hypoxaemic hypercapnia trial, whereas there were no changes (*P* = 0.273 and 0.164, respectively) in the hyperoxaemic hypercapnia trial (Table 2). Apnoea was associated with a general increase in MAP, TPR, IJVP and CPP (State, all *P* < 0.001) that

were greater in the hypoxaemic hypercapnia trial (Trial, *P* = 0.015 to <0.001; Table 2).

Cerebral bioenergetics

Apnoea generally increased gCBF, given equivalent elevations in \dot{Q}_{ICA} and \dot{Q}_{VA} (State, all *P* < 0.001; Fig. 2A–C). Although maximal gCBF was not different between trials (*P* = 0.130), the relative increase was greater during hyperoxaemic hypercapnia (+206 ± 52 *vs.* +83 ± 22%, *P* < 0.001) owing to consistently lower eupnoeic \dot{Q}_{ICA} and \dot{Q}_{VA} (all *P* < 0.001; Fig. 2A–C), probably reflecting hyperventilation-induced hypocapnia-mediated cerebral vasoconstriction (Table 1). Figure 2D illustrates the theoretical changes in gCBF attributable to changes in *P*_{aO₂} (hypo/hyperoxaemia) independent of changes in *P*_{aCO₂}, highlighting the extent to which prevailing hypo/hypercapnia led to an under/overestimation, respectively, in gCBF. Corresponding apnoea-induced increases in gCDO₂ (*P* < 0.001; Fig. 2E) and gCD_{Glu} (*P* = 0.024; Fig. 2F) and reciprocal reductions in O₂ and Glu extraction (all *P* < 0.001; Fig. 2G and H) were also greater in the hyperoxaemic hypercapnia trial. Apnoea generally decreased gCMRO₂ (State, *P* = 0.015; Fig. 2I) and gCMR_{Glu} (State, *P* = 0.023; Fig. 2J), with gCMR_{Glu} generally lower in the hypoxaemic hypercapnia trial (Trial, *P* = 0.044; Fig. 2J).

Oxidative stress

Apnoea generally increased the a–v_D (State, *P* = 0.010–0.015; Table 3) and corresponding net cerebral uptake of ascorbate, α-tocopherol and total LSA (all State, *P* = 0.004; Fig. 3A–C), which were greater in the hypoxaemic hypercapnia trial (Trial, *P* = 0.004–0.046; Fig. 3A–C). This was accompanied by a reduction in the a–v_D (State, *P* = 0.047 to 0.048; Table 3) and reciprocal elevation in the net cerebral output of A^{•-} (State, *P* = 0.020; Fig. 3D) and LOOH (State, *P* = 0.048; Fig. 3E), which was greater for A^{•-} in the hypoxaemic hypercapnia trial (Trial × State, *P* = 0.046; Fig. 3D).

Nitrosative stress

Figure 4 highlights the dynamic interplay and re-apportionment of NO metabolites across the cerebral circulation observable within the constraints of a single a–v transit. The total (plasma + RBC) NO metabolite pool was generally higher in the hyperoxaemic hypercapnia trial (Trial, *P* = 0.044; Table 4 and Fig. 4) owing to the combined effects of elevated plasma (Trial, *P* = 0.010; Table 4 and Fig. 4) and RBC (Trial, *P* = 0.048, Table 4 and Fig. 4) NO₂⁻ that was especially apparent in the

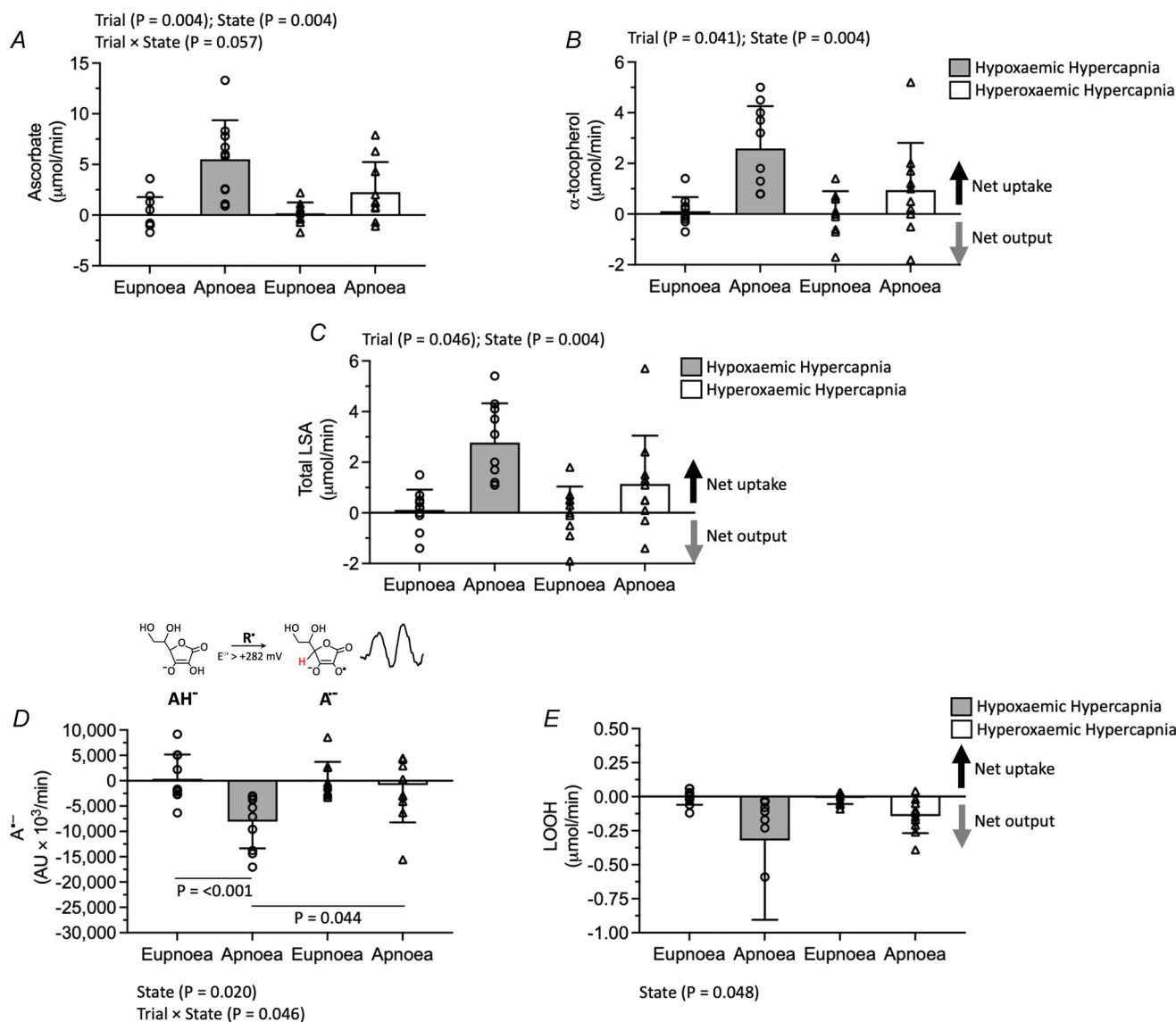


Figure 3. Oxidative stress exchange kinetics
 Values are mean \pm SD based on 10 participants. Circles and triangles denote individual data points for participants during the hypoxaemic hypercapnia and hyperoxaemic hypercapnia trials, respectively. Total lipid soluble antioxidants (LSA) were calculated as the cumulative concentration of α/γ -tocopherol, α/β -carotene, retinol and lycopene. Abbreviations: $A^{\bullet-}$, ascorbate free radical; LOOH, lipid hydroperoxides. Exchange was calculated as the product of global cerebral plasma/serum flow and arterio-jugular venous concentration difference. Positive or negative gradients reflect net cerebral uptake (loss or consumption) or output (gain or formation), respectively. Given that the concentration of ascorbate in human plasma is orders of magnitude greater than any oxidizing free radical combined with the low one-electron reduction potential for the $A^{\bullet-}$ /ascorbate monianion ($\text{AH}^{\bullet-}$) couple ($E^{\circ} = 282 \text{ mV}$) (Williams & Yandell, 1982), any oxidizing species (R^{\bullet}) generated locally within the cerebral circulation will result in the one-electron oxidation of ascorbate to form the distinctive EPR-detectable $A^{\bullet-}$ doublet ($R^{\bullet} + \text{AH}^{\bullet-} \rightarrow \text{A}^{\bullet-} + \text{R-H}$; inset in *D*, with main coupling hydrogen highlighted in red) (Buettner, 1993). Data were analyzed using two-factor (Trial: hypoxaemic hypercapnia vs. hyperoxaemic hypercapnia \times State: eupnoea vs. apnoea) repeated-measures ANOVA. *Post hoc* Bonferroni-corrected Student's paired samples *t* tests were used to locate differences following an interaction. Summary interpretation: despite a greater increase in the net cerebral uptake ($a > v$) of aqueous and lipid-phase antioxidants, the apnoea-induced elevation in the rate of cerebral free radical formation ($v > a$) was selectively greater in the hypoxaemic hypercapnia trial.

Table 3. Oxidative stress

Trial:	Hypoxaemic hypercapnia (n = 10)				Hyperoxaemic hypercapnia (n = 10)			
	Eupnoea		Apnoea		Eupnoea		Apnoea	
	Arterial	Venous	Arterial	Venous	Arterial	Venous	Arterial	Venous
Antioxidants								
Ascorbate (μM)	59.3 ± 11.0	59.2 ± 10.0	61.8 ± 8.9	53.5 ± 6.4	61.0 ± 6.7	60.5 ± 5.3	63.0 ± 5.6	60.0 ± 3.7
Site ($P = 0.007$); Trial × Site ($P = 0.017$); State × Site ($P = 0.015$)	0.2 ± 4.3		8.3 ± 5.6		0.5 ± 4.9		3.0 ± 4.0	
α -Tocopherol (μM)	22.1 ± 3.9	21.7 ± 3.2	24.4 ± 3.0	20.4 ± 3.4	22.5 ± 4.9	22.7 ± 4.1	22.7 ± 2.9	21.3 ± 3.2
Site ($P = 0.008$); State × Site ($P = 0.011$)	0.3 ± 1.5		4.0 ± 2.6		−0.1 ± 4.2		1.4 ± 2.6	
Total LSA (μM)	25.6 ± 3.6	25.2 ± 3.1	28.0 ± 2.6	23.7 ± 3.0	26.0 ± 4.7	26.2 ± 3.9	26.0 ± 2.5	24.4 ± 2.7
Site ($P = 0.006$); State × Site ($P = 0.010$)	0.4 ± 2.1		4.3 ± 2.4		−0.1 ± 4.7		1.6 ± 2.6	
Free radicals								
$\text{A}^{\cdot-}$ (a.u. × 10 ²)	320 ± 107	313 ± 98	344 ± 95	473 ± 127	322 ± 70	333 ± 102	363 ± 143	386 ± 129
State ($P = 0.009$); Site ($P = 0.046$); State × Site ($P = 0.048$)	6 ± 130		−129 ± 96		−12 ± 143		−24 ± 91	
Lipid peroxidation								
LOOH (μM)	1.15 ± 0.17	1.16 ± 0.13	1.22 ± 0.25	1.74 ± 1.20	1.19 ± 0.15	1.25 ± 0.22	1.27 ± 0.18	1.45 ± 0.24
Site ($P = 0.038$); State × Site ($P = 0.045$); State × Site ($P = 0.048$)	−0.01 ± 0.14		−0.52 ± 0.97		−0.07 ± 0.23		−0.18 ± 0.15	

Values are mean ± SD based on 10 participants. Positive or negative a–v_D reflects net cerebral uptake (loss or consumption) or output (gain or formation), respectively. Data were analyzed using three-factor (Trial: hypoxaemic hypercapnia vs. hyperoxaemic hypercapnia × State: eupnoea vs. apnoea × Site: arterial vs. venous) repeated-measures ANOVA. *Post hoc* Bonferroni-corrected Student's paired samples *t* tests were used to locate differences following an interaction. Summary interpretation: despite a general increase in the net cerebral uptake (a > v) of aqueous and lipid-phase antioxidants, apnoea increased the cerebral output (v > a) of free radicals and lipid peroxidants in both trials. Abbreviations: $\text{A}^{\cdot-}$, ascorbate free radical; a–v_D, arterio-jugular venous concentration difference; LOOH, lipid hydroperoxides; LSA, total lipid soluble antioxidants, calculated as the cumulative concentration of α/γ -tocopherol, α/β -carotene, retinol and lycopene.

systemic (a) circulation at eupnoea owing to (preceding) hyperoxic hyperventilation (note that Trial × State × Site interaction was observed only for HbNO, $P = 0.045$). In contrast, HbNO (Trial, $P = 0.002$; Table 4 and Fig. 4) and SNO-Hb (Trial, $P = 0.014$; Table 4 and Fig. 4) were comparatively lower in the hyperoxaemic hypercapnia trial. Apnoea generally decreased total plasma (State, $P = 0.003$; Table 4 and Fig. 4) and RBC (State, $P = 0.042$; Table 4 and Fig. 4) NO primarily owing to a reduction in NO_2^- (plasma: State, $P = 0.003$; Table 4 and Fig. 4; and RBC: State, $P = 0.042$; Table 4 and Fig. 4). This was accompanied by modest elevations in HbNO (Trial × State, $P = 0.024$; Table 4 and Fig. 4) and SNO-Hb (State, $P = 0.036$ and Trial × State, $P = 0.022$; Table 4 and Fig. 4) that were greater in the hypoxaemic hyper-

capnia trial. Corresponding NO metabolite a–v gradients translated into heterogeneous exchange kinetics, with a general (eupnoea + apnoea) net cerebral uptake (a > v) observed for plasma NO_2^- , RSNO and RBC NO_2^- (Fig. 5A, B and D) and net cerebral output of SNO-Hb and HbNO (Fig. 5E and F). Apnoea generally increased total plasma NO uptake (State, $P = 0.012$; Fig. 5C) owing to increased plasma NO_2^- uptake (State, $P = 0.009$; Fig. 5A), with reciprocal elevations observed in SNO-Hb (State, $P = 0.042$; Fig. 5E) and HbNO output that, for the latter, was greater in the hypoxaemic hypercapnia trial (Trial × State, $P = 0.049$; Fig. 5F). Plasma NO_2^- uptake was generally lower (Trial, $P = 0.034$, Fig. 5A) and HbNO output higher (Trial, $P = 0.046$; Fig. 5F) in the hypoxaemic hypercapnia trial.

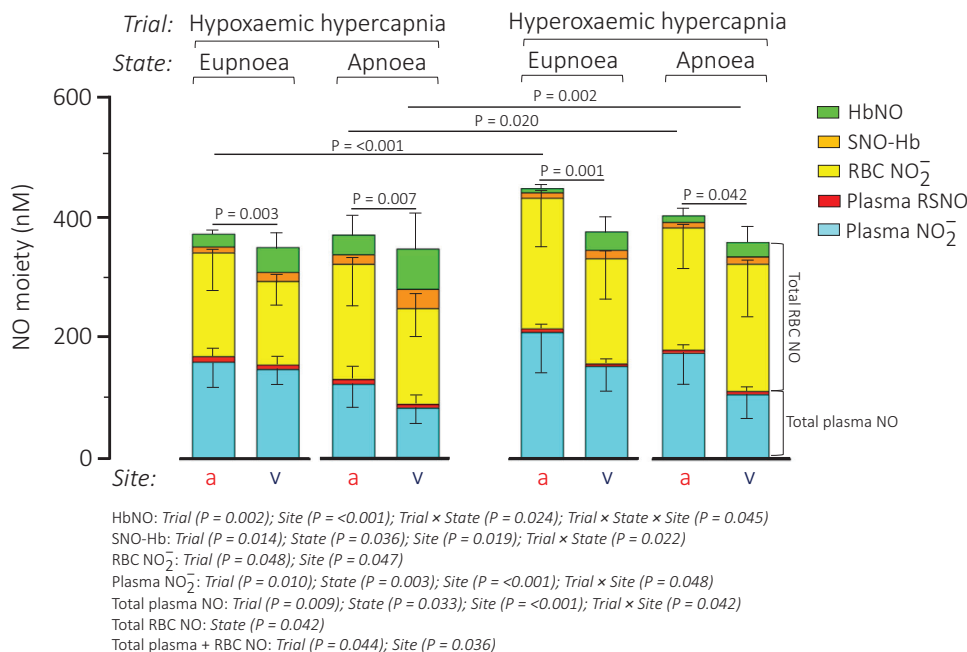


Figure 4. Local distribution of nitric oxide metabolites

Values are mean \pm SD based on 10 participants. Abbreviations: a, arterial; HbNO, nitrosylhaemoglobin; RSNO, S-nitrosothiols; SNO-Hb, S-nitrosohaemoglobin; v, venous. Data were analyzed using three-factor (Trial: hypoxaemic hypercapnia vs. hyperoxaemic hypercapnia \times State: eupnoea vs. apnoea \times Site: arterial vs. venous) repeated-measures ANOVA. *Post hoc* Bonferroni-corrected Student's paired samples *t* tests were used to locate differences following an interaction. Summary interpretation: the NO metabolite pool is in a constant state of flux even within the time constraints of a single a–v transit across the cerebral circulation. Re-apportionment of bioactive moieties between plasma and RBC compartments is related to the combined effects of altered O_2 , carbon dioxide and pH, with the greatest changes observed at eupnoea being attributable to prior hyperoxic hyperventilation in the hyperoxaemic hypercapnia trial. The total (plasma + red blood cell) NO metabolite pool was generally lower in the hypoxaemic hypercapnia trial owing to lower NO_2^- . Apnoea increased plasma NO_2^- uptake ($a > v$) and SNO-Hb/HbNO output ($v > a$), which, for the latter, was selectively elevated in the hypoxaemic hypercapnia trial.

Biological sex differences

Retrospective analyses identified no differences between males and females in apnoea-induced changes in any of the OXNOS exchange (hypoxaemic hypercapnia trial, $P = 0.171$ – 0.914 ; hyperoxaemic hypercapnia trial, $P = 0.114$ – 0.914) or bioenergetic (hypoxaemic hypercapnia trial, $P = 0.610$ – 1.000 ; hyperoxaemic hypercapnia trial, $P = 0.067$ – 0.914) parameters measured. However, given the small effect sizes observed (hypoxaemic hypercapnia trial, 0.000 – 0.539 ; hyperoxaemic hypercapnia trial, 0.067 – 0.539), retrospective power analyzes revealed that we were consistently underpowered, with values ranging from 0.000 to 0.111 and from 0.051 to 0.127 for the hypoxaemic hypercapnia and hyperoxaemic hypercapnia trials, respectively.

Correlational analyzes

Apnoea-induced elevations in A^{*+} and LOOH output were associated with a reduction in plasma NO_2^- uptake in the hypoxaemic hypercapnia trial only ($r = 0.702$,

$P = 0.024$ and $r = 0.629$, $P = 0.041$, respectively). The elevation in gCBF was inversely related to increased LOOH output ($r = -0.811$, $P = 0.004$) and positively related to increased plasma NO_2^- uptake ($r = 0.840$, $P = 0.002$; pooled trials, $r = 0.565$, $P = 0.009$) and RSNO uptake ($r = 0.869$, $P = 0.001$) in the hyperoxaemic hypercapnia trial only. No relationships were observed between altered (apnoea minus eupnoea) exchange in any of the OXNOS metrics and reductions in either gCMRO₂ ($r = 0.109$ – 0.558 , $P = 0.094$ – 0.764) or gCMR_{Glu} ($r = 0.069$ – 0.511 , $P = 0.131$ – 0.850).

Discussion

Local sampling of blood across the cerebral circulation in ultra-elite apnoeists has provided important insight into the mechanisms underlying the redox regulation of cerebral bioenergetic function during the most severe extremes of O_2 demand/ CO_2 production recorded to date in unanaesthetized and otherwise healthy humans (Bailey, Willie et al., 2017). Although it was not possible to fully disassociate changes in P_{aO_2} from

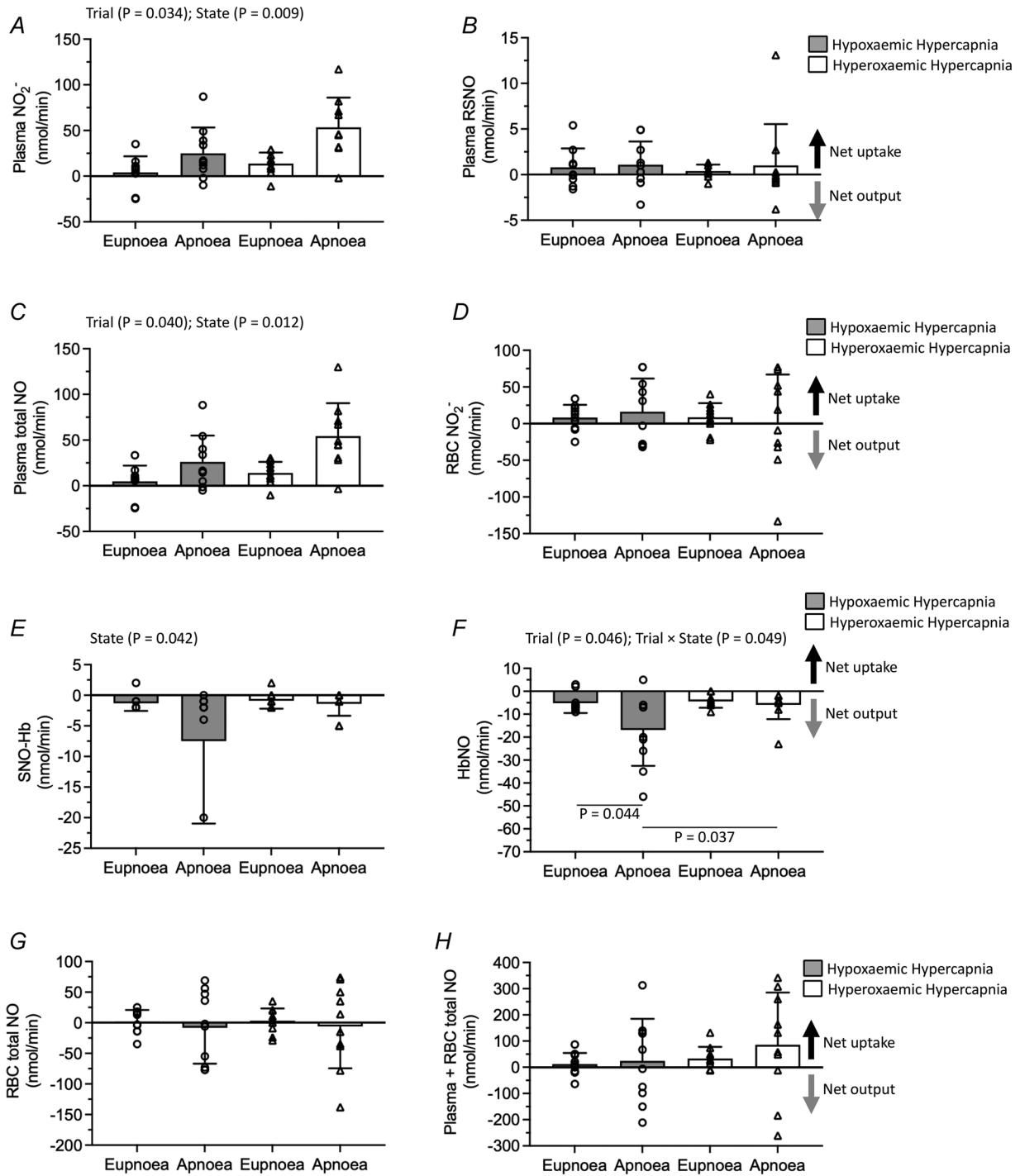


Figure 5. Nitrosative stress exchange kinetics

Values are mean \pm SD based on 10 participants. Circles and triangles denote individual data points for participants during the hypoxaemic hypercapnia and hyperoxaemic hypercapnia trials, respectively. Abbreviations: HbNO, nitrosylhaemoglobin; NO_2^- , nitrite; NO, nitric oxide; RBC, red blood cell; RSNO, S-nitrosothiols; SNO-Hb, S-nitrosohaemoglobin. Exchange was calculated as the product of global cerebral plasma (A–C) or RBC (D–G) or whole blood (H) flow and arterio-jugular venous concentration difference. Positive or negative gradients reflect net cerebral uptake (loss or consumption) or output (gain or formation), respectively. Data were analyzed using two-factor (Trial: hypoxaemic hypercapnia vs. hyperoxaemic hypercapnia \times State: eupnoea vs. apnoea) repeated-measures ANOVA. *Post hoc* Bonferroni-corrected Student's paired samples *t* tests were used to locate differences following an interaction. Summary interpretation: the apnoea-induced increase in cerebral plasma NO_2^- uptake ($a > v$) was selectively blunted and HbNO output ($v > a$) was elevated in the hypoxaemic hypercapnia trial.

Table 4. Nitrosative stress

Trial:	Hypoxaemic hypercapnia (n = 10)				Hyperoxaemic hypercapnia (n = 10)			
	Eupnoea		Apnoea		Eupnoea		Apnoea	
State:								
Site:	Arterial	Venous	Arterial	Venous	Arterial	Venous	Arterial	Venous
Plasma								
NO ₂ ⁻ (nM)	161 ± 45	149 ± 35	124 ± 45	85 ± 34	210 ± 80	154 ± 42	176 ± 55	108 ± 45
Trial (P = 0.010); State (P = 0.003); Site (P < 0.001); Trial × Site (P = 0.048)								
a-v _D (nM)	12 ± 48		39 ± 46		55 ± 55		68 ± 34	
Trial (P = 0.048)								
RSNO (nM)	9 ± 9	7 ± 8	8 ± 11	6 ± 9	6 ± 5	4 ± 4	5 ± 6	5 ± 2
a-v _D (nM)	2 ± 6		2 ± 4		1 ± 3		1 ± 4	
Total NO (nM)	170 ± 43	155 ± 37	132 ± 52	91 ± 39	215 ± 82	159 ± 45	181 ± 58	113 ± 47
Trial (P = 0.009); State (P = 0.033); Site (P < 0.001); Trial × Site (P = 0.042)								
a-v _D (nM)	14 ± 46		41 ± 46		57 ± 55		68 ± 37	
Trial (P = 0.042)								
Red blood cell								
NO ₂ ⁻ (nM)	171 ± 62	138 ± 39	190 ± 71	158 ± 52	216 ± 84	174 ± 65	202 ± 72	210 ± 96
Trial (P = 0.048); Site (P = 0.047)								
a-v _D (nM)	33 ± 64		33 ± 94		42 ± 106		-8 ± 128	
SNO-Hb (nM)	10 ± 3	15 ± 5	16 ± 5	32 ± 30	9 ± 4	14 ± 6	9 ± 3	12 ± 3
Trial (P = 0.014); State (P = 0.036); Site (P = 0.019); Trial × State (P = 0.022)								
a-v _D (nM)	-5 ± 5		-16 ± 31		-5 ± 6		-3 ± 5	
HbNO (nM)	21 ± 5	41 ± 15*	32 ± 20	66 ± 38*	7 ± 3†	30 ± 16*	11 ± 8†	24 ± 17†
Trial (P = 0.002); Site (P < 0.001); Trial × State (P = 0.024); Trial × State × Site (P = 0.045)								
a-v _D (nM)	-20 ± 16		-34 ± 31		-1 ± 13		-29 ± 33†	
Trial × State (P = 0.049)								
Total NO (nM)	202 ± 62	194 ± 47	239 ± 81	256 ± 81	232 ± 81	218 ± 65	222 ± 72	245 ± 103
State (P = 0.042)								
a-v _D (nM)	8 ± 68		-17 ± 120		14 ± 112		-24 ± 139	
Plasma + red blood cell								
Total NO (nM)	371 ± 69	349 ± 50	371 ± 103	347 ± 107	447 ± 96	376 ± 93	403 ± 88	358 ± 134
Trial (P = 0.044); Site (P = 0.036)								
a-v _D (nM)	22 ± 68		24 ± 140		71 ± 85		44 ± 161	

Values are mean ± SD based on 10 participants. Positive or negative a-v_D reflects net cerebral uptake (loss or consumption) or output (gain or formation), respectively. Data were analyzed using three-factor (Trial: hypoxaemic hypercapnia vs. hyperoxaemic hypercapnia × State: eupnoea vs. apnoea × Site: arterial vs. venous) repeated-measures ANOVA. *Post hoc* Bonferroni-corrected Student's paired samples *t* tests were used to locate differences following an interaction. *Different between Site for given Trial and State (P < 0.05); †different between Trial for given State and Site (P < 0.05). Summary interpretation: the total (plasma + red blood cell) NO metabolite pool was lower in the hypoxaemic hypercapnia trial owing primarily to lower NO₂⁻. Apnoea increased plasma NO₂⁻ uptake (a > v) and SNO-Hb/HbNO output (v > a), which for the latter was selectively elevated in the hypoxaemic hypercapnia trial. Abbreviations: a-v_D, arterio-jugular venous concentration difference; HbNO, nitrosylhaemoglobin; NO₂⁻, nitrite; RSNO, S-nitrosothiols; SNO-Hb, S-nitrosohaemoglobin.

P_{aCO_2} , only differential combinations thereof, direct measures of intravascular OXNOS and inclusion of the hyperoxaemic hypercapnia trial designed to ablate hypoxaemia and better distinguish between competing, albeit combinatorial vasoactive stimuli, highlights three novel findings. First, the combined elevation in the net cerebral output of A*⁻ and LOOH observed during apnoea (see Fig. 3D and E), collectively taken to reflect increased free radical-mediated lipid peroxidation, was greater in the hypoxaemic hypercapnia compared

with the hyperoxaemic hypercapnia trial, highlighting a key contribution for hypoxaemia. Second, hypoxaemic hypercapnia coincided with a comparatively lower apnoea-induced elevation in gCBF (see Fig. 2A) and related suppression in plasma NO₂⁻ uptake (see Fig. 5A), implying reduced consumption and delivery of NO, consistent with increased cerebral OXNOS. Finally, apnoea-induced NO₂⁻ uptake (see Fig. 5A) and HbNO output (see Fig. 5F) prevailed in the face of increased SNO-Hb output (see Fig. 5E) and (general) RSNO uptake

(see Fig. 5B), tentatively suggesting NO_2^- reduction as the dominant regulatory mechanism with the capacity to transduce physiological O_2 - CO_2 gradients into graded cerebral vasodilatation.

Hypoxaemic hypercapnia is a key stimulus for cerebral OXNOS

Recently, we documented molecular evidence for structural destabilization of the neurovascular unit, demonstrating increased permeability of the blood-brain barrier at end-apnoea that was selectively greater in the hypoxaemic hypercapnia compared with the hyperoxaemic hypercapnia trial despite comparatively suppressed, albeit concerted vasodilatation (Bailey, Bain et al., 2022). This was originally attributed purely to the 'mechanical' stress imposed by more severe systemic and intracranial hypertension caused by hypoxaemia, potentially encompassing impaired dynamic cerebral autoregulation previously documented in breath-hold divers (Cross et al., 2014) with hyperperfusion-mediated autoregulatory breakthrough, probably compounded by intrathoracic compression and intermittent surges in intrathoracic/systolic pressure triggered by the IBMs. However, the present findings suggest a potentially additive role for 'chemical' stress, taking the form of elevated cerebral OXNOS, to which the human brain has evolved exquisite sensitivity (Bailey, 2019c; Copley et al., 2018).

To do this, we used EPR spectroscopic detection of the distinctive $\text{A}^{\bullet-}$ 'doublet' as a direct biomarker of global free radical formation, with LOOH serving as a distal reactant of lipid peroxidation (Bailey et al., 2018). The finding that net cerebral uptake ($a > v$) of ascorbate, α -tocopherol and (total) LSA was observed during apnoea in both trials and was greater in the hypoxaemic hypercapnia trial (see Fig. 3A-C) was taken to reflect enhanced sacrificial consumption (uptake by brain parenchyma and/or blood-borne reactions during circulatory transit) to constrain chain initiation-propagation reactions. However, this failed to prevent the overall shift in redox imbalance favouring increased free radical-mediated lipid peroxidation, confirmed by equivalent increases in the net cerebral output of $\text{A}^{\bullet-}$ and LOOH ($v > a$), which were elevated selectively in the hypoxaemic hypercapnia trial (see Fig. 3D and E). The greater elevation in $\text{A}^{\bullet-}$ output in the hypoxaemic hypercapnia trial exceeded that predicted by prior modelling owing to more ascorbate available for oxidation (Fall et al., 2018) (given increased consumption), highlighting authentic (i.e. *de novo*) free radical formation. Our measured $\text{A}^{\bullet-}$ gradients in the hypoxaemic hypercapnia trial ($v = 37\% > a$; see Table 3) also exceeded those previously recorded in a separate group of ultra-elite apnoeists ($v = 4\% > a$; Bain, Ainslie

et al., 2018) and were even more marked compared with values documented during vigorous cycling exercise ($v = 12\% > a$; Bailey et al., 2018), helping to place the magnitude of exchange observed in the present study into clearer physiological context.

Although it is conceivable that hypoxaemia, hypercapnia and hyperoxaemia contributed independently towards cerebral oxidative stress and altered bioenergetic function, it was not possible experimentally to differentiate between individual gases (i.e. to disassociate altered P_{aO_2} from P_{aCO_2}), only differential combinations thereof (i.e. end-apnoea hypoxaemic vs. hyperoxaemic hypercapnea). The (P_{aCO_2})-adjusted gCBF findings (Fig. 2D) highlight the extent to which the prevailing hypo/hypercapnia led to an under/overestimation, respectively, in gCBF and, by consequence, $\text{CDO}_2/\text{CD}_{\text{Glu}}$, confirming the heightened sensitivity of the cerebrovasculature to alterations in P_{aCO_2} relative to P_{aO_2} , with the former (hypercapnia) clearly being the dominant stimulus driving apnoea-induced elevation(s) in gCBF.

Hypoxaemia and hyperoxaemia are both independently capable of generating mitochondrial $\text{O}_2^{\bullet-}$ and NO, notwithstanding contributions from extramitochondrial sources, including NADPH and xanthine oxidases, cytochrome P450 enzymes, lipoxygenases and phagocytes, which can propagate oxidative stress further via secondary formation of H_2O_2 , ONOO⁻ and Haber-Weiss/Fenton-catalysed HO[•] (Murphy, 2009; Turrens, 2003). Furthermore, the addition of (hypercapnic) acidosis, common to both trials but, as anticipated, more severe in the hyperoxaemic hypercapnia trial owing to extended breath-hold times (see Table 1), might have compounded oxidation, given the increased bioavailability of molecular CO_2 and H^+ (Dean, 2010; Pryor et al., 2006; Radi, 2022), although we cannot discount the potential reduction in mitochondrial ROS subsequent to (greater) P_{aCO_2} -mediated suppression of CMRO_2 and subsequent electron flux through the ETC. However, the finding that cerebral oxidative stress was markedly elevated in the hypoxaemic hypercapnia trial (see Fig. 3D and E) suggests a key catalytic role for hypoxaemia that far outweighed the additive effects of hyperoxaemia and (more severe) hypercapnia, confirming prior observations in healthy humans, albeit exposed to poikilocapnic (hypocapnic) hypoxia (Bailey et al., 2018; Bailey, Taudorf, Berg, Lundby et al., 2009).

The extent to which cerebral OXNOS represents a physiologically adaptive (molecular signalling) or pathologically maladaptive (structurally damaging) response remains unclear, given the pleiotropic mechanisms underlying redox regulation of cerebral bioenergetic function (Copley et al., 2018), notwithstanding additional complexities associated with differential vasoreactivity of species (Donato et al.,

2010; Richardson et al., 2007; Wray et al., 2009). The finding that oxidative stress was elevated in the face of reduced $gCMRO_2$ and $gCMR_{Glu}$ (see Fig. 2I and J), reflecting an accommodation/reduction of ATP utilization attributable, in part, to the prevailing hypercapnia (Bain et al., 2017), has also been observed in (more) anoxia/hypoxia-tolerant vertebrates and interpreted to reflect an adaptive O_2 -conserving strategy to improve neuronal survival (Bailey, 2019a).

Our group (Bain et al., 2016, 2017) and others (Chen & Pike, 2010; Xu et al., 2011) have previously demonstrated apnoea-induced hypercapnia and resultant acidosis-induced suppression of $CMRO_2$. This has been attributed tentatively to three interrelated mechanisms, including (i) reduced mitochondrial metabolism and/or inhibition of glutamatergic neurotransmission subsequent to (elevated) adenosine A1 receptor activation, (ii) lower glycolytic flux mediated by reduction in phosphofructokinase activity and, albeit to a lesser extent, (iii) Q_{10} -induced reduction in metabolism subsequent to an elevated CBF-induced reduction in brain temperature (Bain et al., 2017). Furthermore, a recent study documented similar reductions in $gCBF$, CDO_2 and $gCMRO_2$ subsequent to elevated (trans)cerebral OXNOS in response to acute 'isocapnic' hyperoxaemia (10 min of 100% O_2) in the absence of any (molecular) evidence of neuronal and parenchymal damage or increased blood-brain barrier permeability (Mattos et al., 2019), suggesting that (physiological) cerebral OXNOS might help to 'titrate' delivery of excess O_2 (and ROS) to protect the cerebrovasculature from structural damage (Bailey, 2019b). Cerebral OXNOS was subsequently ablated following intravenous ascorbate infusion, and bioenergetic function was fully restored (to isocapnic normoxaemic control values) (Mattos et al., 2019), thus lending additional support for the redox regulation of cerebral bioenergetic function.

However, two observations in the present study tentatively suggest that the overall impact of cerebral OXNOS was potentially maladaptive. First, apnoea in the hypoxaemic hypercapnia trial was associated with a lower net uptake of plasma NO_2^- (see Fig. 5A), which implied reduced consumption of NO, potentially tempering vasodilatation (see below). This might reflect oxidative inactivation of NO by $O_2^{\bullet-}$ and/or secondary $LO^{\bullet}/LC^{\bullet}$ formed subsequent to the reductive decomposition of (elevated) LOOH to form $ONOO^-$, collectively taken as evidence for elevated OXNOS ($O_2^{\bullet-}/LO^{\bullet}/LC^{\bullet} + NO \xrightarrow{k \sim 10^9 \text{ M/s}} ONOO^-$) (Bailey et al., 2004). Second, our prior research has demonstrated that apnoea induced mild disruption of the blood-brain barrier and increased neuronal-gliovascular reactivity, which were consistently greater in the hypoxaemic hypercapnia trial (Bailey, Bain et al., 2022) when cerebral OXNOS was

most marked, stands testament to the thermodynamic potential of radicals to cause structural damage to the cerebrovasculature which is not unreasonable given its histological vulnerability (Bailey, 2019c; Copley et al., 2018).

Nitric oxide metabolites and vasoregulation

Our findings highlight that the NO metabolite pool is in a perpetual state of dynamic flux even within the time constraints of a single a-v transit and that metabolite re-apportionment between plasma and RBC compartments is not related solely to changes in O_2 but also involves CO_2 and pH (see Fig. 4). By measuring corresponding gradients of NO_2^- and SNO-Hb, the principal metabolites capable of transducing NO bioactivity within the cerebral microcirculation (Cosby et al., 2003; Jia et al., 1996; Reynolds et al., 2023), we sought to determine whether differential changes could further inform the mechanism(s) underlying cerebral vasodilatation across the $P_{aO_2}-P_{aCO_2}$ continuum. Both metabolites probably originated from the combined effects of apnoea-induced elevations in shear-mediated conduit vessel endothelial (Dimmeler et al., 1999), neuronal (O'Gallagher et al., 2022) NO synthase bioactivation and transpulmonary S-nitrosylation (Jia et al., 1996). However, their respective roles in NO signalling and cerebral bioenergetic function remain widely contested, albeit unified by allosterically coupled Hb deoxygenation and acidic disproportionation (Gladwin & Schechter, 2004).

The direction and magnitude of gradients observed in the present study are generally more consistent with those predicted by the NO_2^- reductase (as opposed to the SNO-Hb) hypothesis. In support, systemic (a) plasma NO_2^- fell during apnoea (see Table 4 and Fig. 4) and was accompanied by a concomitant increase in net uptake (see Fig. 5A), implying consumption from artery to vein ($a > v$), although we cannot discount consistently elevated NO_2^- formation on the arterial side owing to elevated NOS activity. Plasma NO_2^- consumption was elevated in the hyperoxaemic hypercapnia trial (see Fig. 3D and E), coinciding with the greatest elevation in $gCBF$ (see Fig. 2A) and where the total NO metabolite pool was greatest (see Fig. 4). This was accompanied by NO formation with concomitant output ($v > a$) of HbNO (see Fig. 5F), albeit suppressed in the hyperoxaemic hypercapnia trial consistent with the prevailing S_{O_2} , given that hyperoxaemia persisted at end-apnoea (see Table 1), culminating in an overall net gain in NO metabolites (see Fig. 4).

These findings were taken to reflect a combination of deoxyHb-mediated reduction of NO_2^- in the RBC (see reaction in Introduction) and acidic disproportionation

subsequent to marked hypercapnia-induced acidosis. Local formation of NO, potentially compounded by the observed increase in ascorbate consumption (Ladurner et al., 2012), binds to vicinal deoxyHb to yield HbNO [$\text{NO} + \text{HbFe}^{2+} \xrightarrow{k \sim 0.18 \text{ M/s}} \text{HbFe}^{2+} \text{NO (HbNO)}$] and, to a lesser extent, the intermediate nitrosating species dinitrogen trioxide, which can escape the RBC to effect graded vasodilatation (Cosby et al., 2003). The gradients observed (see Table 4) reproduce those previously documented across the exercising human forearm circulation and NO_2^- infusion that originally informed the NO_2^- reductase hypothesis (Cosby et al., 2003; Gladwin et al., 2000). More recently, similar gradients were documented across the cerebral circulation at rest and in response to acute exercise during hypocapnic hypoxia (Bailey, Rasmussen et al., 2017). Recent evidence in rodents also supports NO_2^- reduction in astrocyte mitochondria via sulphite oxidase as the primary mechanism underlying intraparenchymal hypoxic vasodilatation (Christie et al., 2023).

In contrast, the finding that apnoea stimulated SNO-Hb output ($v > a$; see Fig. 5E) and RSNO uptake ($a > v$; see Fig. 5B) tentatively argues against the SNO-Hb hypothesis, because the gradients observed were diametrically opposed to those originally predicted (McMahon et al., 2002), yet consistent with the observations of other research laboratories (Gladwin et al., 2002; Wang et al., 2006). We would have expected an allosterically mediated release from a to v during circulatory transit, resulting in a drop in the RBC and corresponding rise in plasma RSNO in the venous circulation, consistent with SNO-Hb consumption ($a > v$) and RSNO delivery ($v > a$) during local deoxygenation. Nevertheless, the gradients observed consistently reflected SNO-Hb formation ($v > a$; see Fig. 5E) and RSNO consumption ($a > v$; see Fig. 5B), which, in the former, was compounded further during apnoea and unrelated to the increase in gCBF or to any of the bioenergetic metrics.

Experimental limitations

Several limitations warrant consideration to provide a balanced appraisal of our findings. As highlighted, it was not possible to disassociate changes in P_{aO_2} from P_{aCO_2} , only differential combinations thereof, given the inability to 'match' eupnoeic hypocapnia/end-apnoea hypercapnia across trials that was evidently more severe in the hyperoxaemic hypercapnia trial (see Table 1) owing to (prior) hyperoxic hyperventilation and extended breath-hold times. It is unfortunate that we did not include a third trial, preceded by normoxaemic hyperventilation to achieve end-apnoea hypoxaemic normocapnia. Future studies using the specialist technique of dynamic end-tidal forcing (Willie et al., 2015) will help to distinguish between competing stimuli across the P_{O_2} - P_{CO_2} continuum (e.g. isocapnic hypo/hyperoxia vs. isoxic hypo/hypercapnia).

It was equally unfortunate that we did not measure plasma 3-nitrotyrosine owing to inadequate sample volume; its elevation would indirectly have confirmed increased ONOO^- formation subsequent to oxidative inactivation of NO underlying OXNOS, consistent with our prior observations in hypoxia (Bailey et al., 2011). Likewise, the profiling of end-point NO metabolite gradients (see Table 4), although informative, fails to identify unequivocally the temporal kinetics (see below) and specific NO moieties responsible for conserving bioactivity and mechanism(s) underpinning vasoregulation. This was a highly dynamic study and thus a true steady state transcerebral OXNOS exchange kinetic was never attained. Although it would have been informative to perform serial measurements to assess the temporal dynamics of exchange kinetics as hypo/hyperoxaemic hypercapnic stress evolves over the course of (each) apnoea, we were bound by ethical constraints associated with excessive blood volume loss, given that this study adopted a repeated-measures design. Owing to logistical constraints, we also failed to assess (potential) contributions of RBC ATP signalling to cerebral hypoxic vasodilatation subsequent to endothelial $\text{P}_{2\text{Y}}$ receptor-mediated endothelial nitric oxide synthase activation (Dietrich et al., 2000; Ellsworth et al., 1995). Despite all blood samples being treated identically, exposure to room air and cooling, unavoidable consequences associated with preparation and batch analysis *ex vivo*, have the potential to alter SNO-Hb/HbNO apportionment (McMahon et al., 2002).

From an experimental design perspective, although prospective power calculations based on our prior research (Bain, Ainslie et al., 2018) helped to inform the present approach, we acknowledge that the small sample sizes might have limited our ability to detect treatment effects, albeit challenging to perform large-scale invasive studies of this nature. Furthermore, future studies need to consider the inclusion of females to (better) investigate sex differences in the redox regulation of cerebral bioenergetic function, given that our retrospective analyses identified that we were consistently underpowered to detect treatment effects. Our prospective calculations indicate that studies will need to include (on average) 935 participants per group (hypoxaemic hypercapnia trial, 58–3663 participants; hyperoxaemic hypercapnia trial, 46–3663 participants) to detect *a priori* differences, given observed effect sizes and power ($1 - \beta$ of 0.80 at $P < 0.05$), a significant and highly unlikely undertaking, given the invasive nature of catheterization.

An additional caveat, despite excellent agreement between confluent intra- and extracranial blood velocities, relates to the unavoidable estimation of changes in \dot{Q}_{ICA} and \dot{Q}_{VA} (see Fig. 2A and B) based on linear extrapolation of changes in MCAv and PCAv owing to increased severity of IBMs at maximal apnoea. Likewise,

although we assumed bilateral \dot{Q}_{ICA} and \dot{Q}_{VA} symmetry when calculating gCBF, a recent study identified that this (unilateral) approach yields a mean measurement error of 5% (when determining the relative gCBF response to hypoxia), with individual errors as high as 37% and greatest in ICAs and VAs with the lowest resting blood flow owing to a ratio-scaling problem (Friend et al., 2021). When synchronous bilateral assessments of extra/intracranial flows/velocities are not feasible (e.g. owing to ultrasound interference and Duplex probe space constraints, as encountered in the present study), future researchers need to consider selecting those extracranial arteries with the highest resting normoxic blood flow after prescreening of both left and right vessels, in an attempt to minimize (unilateral) measurement error. This is an important consideration, given its direct impact on all (Fick-derived) exchange measures.

Equally, we did not perform a dedicated validation study to determine whether the Modelflow algorithm is valid for estimation of SV, \dot{Q} and TPR or blood pressure (see Table 2), especially towards the end of the apnoeas when IBMs are most severe (see Fig. 1B). However, we have previously observed excellent agreement between (non-invasive, indirect) finger photoplethysmographic and (invasive, direct) intra-arterial measurement of blood pressure ($r^2 = 0.59$, $P \leq 0.001$; unpublished findings). Equally, previous studies have demonstrated excellent agreement between measured SV (Doppler ultrasound) and Modelflow estimates in the resting supine state, albeit any acute elevation in TPR (such as that observed at end-apnoea in the present study; see Table 2) leads to consistent overestimation of SV, thus warranting caution when interpreting findings (Dyson et al., 2010).

Finally, future studies should also consider interventional (pharmacological) approaches that include targeted antioxidant prophylaxis to better define the bioenergetic implications of altered cerebral OXNOS. In addition to ascorbate infusion (Mattos et al., 2019), this might also include (for example) the orally available mitochondrial-targeted coenzyme Q10 (MitoQ) in humans (Murphy & Hartley, 2018) and potential future application of a newly synthesized class of β -phosphorylated linear nitrones (Mito-PPNs) in animal models (Culcasi et al., 2023), given their superior ability to scavenge $O_2^{\cdot-}$, HO^{\cdot} and H_2O_2 .

Conclusions

Local sampling of blood across the cerebral circulation in world-class apnoeists has highlighted a key catalytic role for hypoxaemic hypercapnia in cerebral OXNOS and tentatively identified NO_2^- reduction as the dominant mechanism underlying NO vasoregulation with the

capacity to transduce physiological O_2 - CO_2 gradients into graded cerebral vasodilatation. Collectively, these findings highlight the dynamic interplay that takes place between free radicals and NO metabolites during a single a-v transit across the cerebral circulation and corresponding implications for cerebral bioenergetic function that might help to inform interventions designed to optimize tissue oxygenation in the critically ill.

References

- Bailey, D. M. (2019a). Oxygen and brain death; back from the brink. *Experimental Physiology*, **104**(12), 1769–1779.
- Bailey, D. M. (2019b). Oxygen is rocket fuel for the human brain; a radical perspective! *The Journal of Physiology*, **597**(3), 659–660.
- Bailey, D. M. (2019c). Oxygen, evolution and redox signalling in the human brain; quantum in the quotidian. *The Journal of Physiology*, **597**(1), 15–28.
- Bailey, D. M., Bain, A. R., Hoiland, R. L., Barak, O. F., Drvis, I., Hirtz, C., Lehmann, S., Marchi, N., Janigro, D., Macleod, D. B., Ainslie, P. N., & Dujic, Z. (2022). Hypoxemia increases blood-brain barrier permeability during extreme apnea in humans. *Journal of Cerebral Blood Flow and Metabolism*, **42**(6), 1120–1135.
- Bailey, D. M., Brugniaux, J. V., Filippini, T., Marley, C. J., Stacey, B., Soria, R., Rimoldi, S. F., Cerny, D., Rexhaj, E., Pratali, L., Salmón, C. S., Murillo Jáuregui, C., Villena, M., Smirl, J. D., Ogoh, S., Pietri, S., Scherrer, U., & Sartori, C. (2019). Exaggerated systemic oxidative-inflammatory-nitrosative stress in chronic mountain sickness is associated with cognitive decline and depression. *The Journal of Physiology*, **597**(2), 611–629.
- Bailey, D. M., Culcasi, M., Filippini, T., Brugniaux, J. V., Stacey, B. S., Marley, C. J., Soria, R., Rimoldi, S. F., Cerny, D., Rexhaj, E., Pratali, L., Salmon, C. S., Jauregui, C. M., Villena, M., Villafuerte, F., Rockenbauer, A., Pietri, S., Scherrer, U., & Sartori, C. (2022). EPR spectroscopic evidence of iron-catalysed free radical formation in chronic mountain sickness: Dietary causes and vascular consequences. *Free Radical Biology & Medicine*, **184**, 99–113.
- Bailey, D. M., Evans, K. A., Mceneny, J., Young, I. S., Hullin, D. A., James, P. E., Ogoh, S., Ainslie, P. N., Lucchesi, C., Rockenbauer, A., Culcasi, M., & Pietri, S. (2011). Exercise-induced oxidative–nitrosative stress is associated with impaired dynamic cerebral autoregulation and blood–brain barrier leakage. *Experimental Physiology*, **96**(11), 1196–1207.
- Bailey, D. M., Rasmussen, P., Evans, K. A., Bohm, A. M., Zaar, M., Nielsen, H. B., Brassard, P., Nordsborg, N. B., Homann, P. H., Raven, P. B., McEneny, J., Young, I. S., McCord, J. M., & Secher, N. H. (2018). Hypoxia compounds exercise-induced free radical formation in humans; partitioning contributions from the cerebral and femoral circulation. *Free Radical Biology & Medicine*, **124**, 104–113.

- Bailey, D. M., Rasmussen, P., Overgaard, M., Evans, K. A., Bohm, A. M., Seifert, T., Brassard, P., Zaar, M., Nielsen, H. B., Raven, P. B., & Secher, N. H. (2017). Nitrite and S-Nitrosohemoglobin exchange across the human cerebral and femoral circulation: Relationship to basal and exercise blood flow responses to hypoxia. *Circulation*, **135**(2), 166–176.
- Bailey, D. M., Taudorf, S., Berg, R. M. G., Jensen, L. T., Lundby, C., Evans, K. A., James, P. E., Pedersen, B. K., & Moller, K. (2009). Transcerebral exchange kinetics of nitrite and calcitonin gene-related peptide in acute mountain sickness: Evidence against trigeminovascular activation? *Stroke*, **40**(6), 2205–2208.
- Bailey, D. M., Taudorf, S., Berg, R. M. G., Lundby, C., Mcceneny, J., Young, I. S., Evans, K. A., James, P. E., Shore, A., Hullin, D. A., Mccord, J. M., Pedersen, B. K., & Möller, K. (2009). Increased cerebral output of free radicals during hypoxia: Implications for acute mountain sickness? *American Journal of Physiology-Regulatory, Integrative and Comparative Physiology*, **297**(5), R1283–R1292.
- Bailey, D. M., Willie, C. K., Hoiland, R. L., Bain, A. R., MacLeod, D. B., Santoro, M. A., DeMasi, D. K., Andrijanic, A., Mijacika, T., Barak, O. F., Dujic, Z., & Ainslie, P. N. (2017). Surviving without oxygen: How low can the human brain go? *High Altitude Medicine & Biology*, **18**, 73–79.
- Bailey, D. M., Young, I. S., Mcceneny, J., Lawrenson, L., Kim, J., Barden, J., & Richardson, R. S. (2004). Regulation of free radical outflow from an isolated muscle bed in exercising humans. *American Journal of Physiology-Heart and Circulatory Physiology*, **287**(4), H1689–H1699.
- Bain, A. R., Ainslie, P. N., Barak, O. F., Hoiland, R. L., Drvis, I., Mijacika, T., Bailey, D. M., Santoro, A., Demasi, D. K., Dujic, Z., & Macleod, D. B. (2017). Hypercapnia is essential to reduce the cerebral oxidative metabolism during extreme apnea in humans. *Journal of Cerebral Blood Flow and Metabolism*, **37**(9), 3231–3242.
- Bain, A. R., Ainslie, P. N., Hoiland, R. L., Barak, O. F., Cavar, M., Drvis, I., Stenbridge, M., Macleod, D. M., Bailey, D. M., Dujic, Z., & Macleod, D. B. (2016). Cerebral oxidative metabolism is decreased with extreme apnoea in humans; impact of hypercapnia. *The Journal of Physiology*, **594**(18), 5317–5328.
- Bain, A. R., Ainslie, P. N., Hoiland, R. L., Barak, O. F., Drvis, I., Stenbridge, M., Macleod, D. M., Mcceneny, J., Stacey, B. S., Tuailon, E., Marchi, N., De Maudave, A. F., Dujic, Z., Macleod, D. B., & Bailey, D. M. (2018). Competitive apnea and its effect on the human brain: Focus on the redox regulation of blood-brain barrier permeability and neuronal-parenchymal integrity. *Federation of American Societies for Experimental Biology Journal*, **32**(4), 2305–2314.
- Bain, A. R., Drvis, I., Dujic, Z., Macleod, D. B., & Ainslie, P. N. (2018). Physiology of static breath holding in elite apneists. *Experimental Physiology*, **103**(5), 635–651.
- Buettner, G. R. (1993). The pecking order of free radicals and antioxidants: Lipid peroxidation, α -tocopherol, and ascorbate. *Archives of Biochemistry and Biophysics*, **300**(2), 535–543.
- Caldwell, H. G., Carr, J. M. J. R., Minhas, J. S., Swenson, E. R., & Ainslie, P. N. (2021). Acid-base balance and cerebrovascular regulation. *The Journal of Physiology*, **599**(24), 5337–5359.
- Catignani, G. L., & Bieri, J. G. (1983). Simultaneous determination of retinol and α -tocopherol in serum or plasma by liquid chromatography. *Clinical Chemistry*, **29**(4), 708–712.
- Chandel, N. S., Maltepe, E., Goldwasser, E., Mathieu, C. E., Simon, M. C., & Schumacker, P. T. (1998). Mitochondrial reactive oxygen species trigger hypoxia-induced transcription. *Proceedings of the National Academy of Sciences USA*, **95**(20), 11715–11720.
- Chen, J. J., & Pike, G. B. (2010). Global cerebral oxidative metabolism during hypercapnia and hypocapnia in humans: Implications for BOLD fMRI. *Journal of Cerebral Blood Flow and Metabolism*, **30**(6), 1094–1099.
- Christie, I. N., Theparambil, S. M., Braga, A., Doronin, M., Hosford, P. S., Brazhe, A., Mascarenhas, A., Nizari, S., Hadjihambi, A., Wells, J. A., Hobbs, A., Semyanov, A., Abramov, A. Y., Angelova, P. R., & Gourine, A. V. (2023). Astrocytes produce nitric oxide via nitrite reduction in mitochondria to regulate cerebral blood flow during brain hypoxia. *Cell Reports*, **42**(12), 113514.
- Cobley, J. N., Fiorello, M. L., & Bailey, D. M. (2018). 13 reasons why the brain is susceptible to oxidative stress. *Redox Biology*, **15**, 490–503.
- Cosby, K., Partovi, K. S., Crawford, J. H., Patel, R. P., Reiter, C. D., Martyr, S., Yang, B. K., Waclawiw, M. A., Zalos, G., Xu, X., Huang, K. T., Shields, H., Kim-Shapiro, D. B., Schechter, A. N., Cannon, R. O., & Gladwin, M. T. (2003). Nitrite reduction to nitric oxide by deoxyhemoglobin vasodilates the human circulation. *Nature Medicine*, **9**(12), 1498–1505.
- Coverdale, N. S., Gati, J. S., Opalevych, O., Perrotta, A., & Shoemaker, J. K. (2014). Cerebral blood flow velocity underestimates cerebral blood flow during modest hypercapnia and hypocapnia. *Journal of Applied Physiology*, **117**(10), 1090–1096.
- Cross, T. J., Kavanagh, J. J., Breskovic, T., Johnson, B. D., & Dujic, Z. (2014). Dynamic cerebral autoregulation is acutely impaired during maximal apnoea in trained divers. *PLoS ONE*, **9**(2), e87598.
- Culcasi, M., Delehedde, C., Esgulian, M., Cassien, M., Chocry, M., Rockenbauer, A., Pietri, S., & Th  tiot-Laurent, S. (2023). New biocompatible β -phosphorylated linear nitrones targeting mitochondria: Protective effect in apoptotic cells. *Chemical Biology Chemistry*, **24**(8), e202200749.
- Dean, J. B. (2010). Hypercapnia causes cellular oxidation and nitrosation in addition to acidosis: Implications for CO₂ chemoreceptor function and dysfunction. *Journal of Applied Physiology*, **108**(6), 1786–1795.
- Dietrich, H. H., Ellsworth, M. L., Sprague, R. S., & Dacey, R. G. (2000). Red blood cell regulation of microvascular tone through adenosine triphosphate. *American Journal of Physiology-Heart and Circulatory Physiology*, **278**(4), H1294–H1298.

- Dimmeler, S., Fleming, I., Fisslthaler, B., Hermann, C., Busse, R., & Zeiher, A. M. (1999). Activation of nitric oxide synthase in endothelial cells by Akt-dependent phosphorylation. *Nature*, **399**(6736), 601–605.
- Donato, A. J., Uberoi, A., Bailey, D. M., Walter Wray, D., & Richardson, R. S. (2010). Exercise-induced brachial artery vasodilation: Effects of antioxidants and exercise training in elderly men. *American Journal of Physiology-Heart and Circulatory Physiology*, **298**(2), H671–H678.
- Duranteau, J., Chandel, N. S., Kulisz, A., Shao, Z., & Schumacker, P. T. (1998). Intracellular signalling by reactive oxygen species during hypoxia in cardiomyocytes. *Journal of Biological Chemistry*, **273**(19), 11619–11624.
- Dyson, K. S., Shoemaker, J. K., Arbeille, P., & Hughson, R. L. (2010). Modelflow estimates of cardiac output compared with Doppler ultrasound during acute changes in vascular resistance in women. *Experimental Physiology*, **95**(4), 561–568.
- Ellsworth, M. L., Forrester, T., Ellis, C. G., & Dietrich, H. H. (1995). The erythrocyte as a regulator of vascular tone. *American Journal of Physiology-Heart Circulatory Physiology*, **269**(6), H2155–H2161.
- Fall, L., Brugniaux, J. V., Davis, D., Marley, C. J., Davies, B., New, K. J., Mценeny, J., Young, I. S., & Bailey, D. M. (2018). Redox-regulation of haemostasis in hypoxic exercising humans: A randomised double-blind placebo-controlled antioxidant study. *The Journal of Physiology*, **596**(20), 4879–4891.
- Friend, A. T., Rogan, M., Rossetti, G. M. K., Lawley, J. S., Mullins, P. G., Sandoo, A., Macdonald, J. H., & Oliver, S. J. (2021). Bilateral regional extracranial blood flow regulation to hypoxia and unilateral duplex ultrasound measurement error. *Experimental Physiology*, **106**(7), 1535–1548.
- Gladwin, M. T., & Schechter, A. N. (2004). NO contest: Nitrite versus S-nitroso-hemoglobin. *Circulation Research*, **94**(7), 851–855.
- Gladwin, M. T., Shelhamer, J. H., Schechter, A. N., Pease-Fye, M. E., Waclawiw, M. A., Panza, J. A., Ognibene, F. P., & Cannon, R. O. (2000). Role of circulating nitrite and S-nitrosohemoglobin in the regulation of regional blood flow in humans. *Proceedings of the National Academy of Sciences of the United States of America*, **97**(21), 11482–11487.
- Gladwin, M. T., Wang, X., Reiter, C. D., Yang, B. K., Vivas, E. X., Bonaventura, C., & Schechter, A. N. (2002). S-Nitrosohemoglobin is unstable in the reductive erythrocyte environment and lacks O₂/NO-linked allosteric function. *The Journal of Biological Chemistry*, **277**(31), 27818–27828.
- Guzy, R. D., Hoyos, B., Robin, E., Chen, H., Liu, L., Mansfield, K. D., Simon, M. C., Hammerling, U., & Schumacker, P. T. (2005). Mitochondrial complex III is required for hypoxia-induced ROS production and cellular oxygen sensing. *Cell Metabolism*, **1**(6), 401–408.
- Hoiland, R. L., Ainslie, P. N., Bain, A. R., Macleod, D. B., Stembridge, M., Drvis, I., Madden, D., Barak, O., Macleod, D. M., & Dujic, Z. (2017). Beta1-Blockade increases maximal apnea duration in elite breath-hold divers. *Journal of Applied Physiology*, **122**(4), 899–906.
- Hoiland, R. L., Bain, A. R., Tymko, M. M., Rieger, M. G., Howe, C. A., Willie, C. K., Hansen, A. B., Flück, D., Wildfong, K. W., Stembridge, M., Subedi, P., Anholm, J., & Ainslie, P. N. (2017). Adenosine receptor-dependent signaling is not obligatory for normobaric and hypobaric hypoxia-induced cerebral vasodilation in humans. *Journal of Applied Physiology*, **122**(4), 795–808.
- Hoiland, R. L., Caldwell, H. G., Carr, J. M. J. R., Howe, C. A., Stacey, B. S., Dawkins, T., Wakeham, D. J., Tremblay, J. C., Tymko, M. M., Patrician, A., Smith, K. J., Sekhon, M. S., Macleod, D. B., Green, D. J., Bailey, D. M., & Ainslie, P. N. (2022). Nitric oxide contributes to cerebrovascular shear-mediated dilatation but not steady-state cerebrovascular reactivity to carbon dioxide. *The Journal of Physiology*, **600**(6), 1385–1403.
- Hoiland, R. L., Macleod, D. B., Stacey, B. S., Caldwell, H. G., Howe, C. A., Nowak-Flück, D., Carr, J. M., Tymko, M. M., Coombs, G. B., Patrician, A., Tremblay, J. C., Van Mierlo, M., Gasho, C., Stembridge, M., Sekhon, M. S., Bailey, D. M., & Ainslie, P. N. (2023). Hemoglobin and cerebral hypoxic vasodilation in humans: Evidence for nitric oxide-dependent and S-nitrosothiol mediated signal transduction. *Journal of Cerebral Blood Flow and Metabolism*, **43**(9), 1519–1531.
- Hoiland, R. L., Tymko, M. M., Bain, A. R., Wildfong, K. W., Montealeone, B., & Ainslie, P. N. (2016). Carbon dioxide-mediated vasomotion of extra-cranial cerebral arteries in humans: A role for prostaglandins? *The Journal of Physiology*, **594**(12), 3463–3481.
- Huang, Z. (2005). Enzymatic function of hemoglobin as a nitrite reductase that produces NO under allosteric control. *Journal of Clinical Investigation*, **115**(8), 2099–2107.
- Jia, L. i., Bonaventura, C., Bonaventura, J., & Stamler, J. S. (1996). S-nitrosohaemoglobin: A dynamic activity of blood involved in vascular control. *Nature*, **380**(6571), 221–226.
- Katona, M., Gladwin, M. T., & Straub, A. C. (2023). Flipping off and on the redox switch in the microcirculation. *Annual Review of Physiology*, **85**(1), 165–189.
- Kety, S. S., & Schmidt, C. F. (1948). The effects of altered arterial tensions of carbon dioxide and oxygen on cerebral blood flow and cerebral oxygen consumption of normal young men. *Journal of Clinical Investigation*, **27**(4), 484–492.
- Ladurner, A., Schmitt, C. A., Schachner, D., Atanasov, A. G., Werner, E. R., Dirsch, V. M., & Heiss, E. H. (2012). Ascorbate stimulates endothelial nitric oxide synthase enzyme activity by rapid modulation of its phosphorylation status. *Free Radical Biology & Medicine*, **52**, 2082–2090.
- Mattos, J. D., Campos, M. O., Rocha, M. P., Mansur, D. E., Rocha, H. N. M., Garcia, V. P., Batista, G., Alvares, T. S., Oliveira, G. V., Souza, M. V., Videira, R. L. R., Rocha, N. G., Secher, N. H., Nóbrega, A. C. L., & Fernandes, I. A. (2019). Human brain blood flow and metabolism during isocapnic hyperoxia: the role of reactive oxygen species. *The Journal of Physiology*, **597**(3), 741–755.
- McMahon, T. J., Moon, R. E., Lusching, B. P., Carraway, M. S., Stone, A. E., Stolp, B. W., Gow, A. J., Pawloski, J. R., Watke, P., Singel, D. J., Piantadosi, C. A., & Stamler, J. S. (2002). Nitric oxide in the human respiratory cycle. *Nature Medicine*, **8**(7), 711–717.

- Murphy, M. P. (2009). How mitochondria produce reactive oxygen species. *The Biochemical Journal*, **417**(1), 1–13.
- Murphy, M. P., & Hartley, R. C. (2018). Mitochondria as a therapeutic target for common pathologies. *Nature Reviews Drug Discovery*, **17**(12), 865–886.
- Myerson, A. (1932). Internal jugular venous pressure in man: Its relationship to cerebrospinal fluid and carotid arterial pressures. *Archives of Neurology and Psychiatry*, **27**(4), 836–846.
- Nauser, T., & Koppenol, W. H. (2002). The rate constant of the reaction of superoxide with nitrogen monoxide: Approaching the diffusion limit. *Journal of Physical Chemistry A*, **106**(16), 4084–4086.
- O’Gallagher, K., Rosentreter, R. E., Elaine Soriano, J., Roomi, A., Saleem, S., Lam, T., Roy, R., Gordon, G. R., Raj, S. R., Chowienczyk, P. J., Shah, A. M., & Phillips, A. A. (2022). The effect of a neuronal nitric oxide synthase inhibitor on neurovascular regulation in humans. *Circulation Research*, **131**(12), 952–961.
- Pawloski, J. R., Hess, D. T., & Stamler, J. S. (2001). Export by red blood cells of nitric oxide bioactivity. *Nature*, **409**(6820), 622–626.
- Pinder, A. G., Rogers, S. C., Khalatbari, A., Ingram, T. E., & James, P. E. (2009). The measurement of nitric oxide and its metabolites in biological samples by ozone-based chemiluminescence. *Methods in Molecular Biology*, **476**, 10–27.
- Premont, R. T., Reynolds, J. D., Zhang, R., & Stamler, J. S. (2020). Role of nitric oxide carried by hemoglobin in cardiovascular physiology: Developments on a three-gas respiratory cycle. *Circulation Research*, **126**(1), 129–158.
- Pryor, W. A., Houk, K. N., Foote, C. S., Fukuto, J. M., Ignarro, L. J., Squadrito, G. L., & Davies, K. J. A. (2006). Free radical biology and medicine: It’s a gas, man! *American Journal of Physiology-Regulatory, Integrative and Comparative Physiology*, **291**(3), R491–R511.
- Radi, R. (2022). Interplay of carbon dioxide and peroxide metabolism in mammalian cells. *The Journal of Biological Chemistry*, **298**(9), 102358.
- Reynolds, J. D., Posina, K., Zhu, L., Jenkins, T., Matto, F., Hausladen, A., Kashyap, V., Schilz, R., Zhang, R., Mannick, J., Klickstein, L., Premont, R. T., & Stamler, J. S. (2023). Control of tissue oxygenation by S-nitrosohemoglobin in human subjects. *Proceedings of the National Academy of Sciences of the United States of America*, **120**(9), e2220769120.
- Richardson, R. S., Donato, A. J., Uberoi, A., Wray, D. W., Lawrenson, L., Nishiyama, S., & Bailey, D. M. (2007). Exercise-induced brachial artery vasodilation: Role of free radicals. *American Journal of Physiology-Heart and Circulatory Physiology*, **292**(3), H1516–H1522.
- Rogers, S. C., Khalatbari, A., Gapper, P. W., Frenneaux, M. P., & James, P. E. (2005). Detection of human red blood cell-bound nitric oxide. *Journal of Biological Chemistry*, **280**(29), 26720–26728.
- Scheinberg, P., & Stead, E. A. (1949). The cerebral blood flow in male subjects as measured by the nitrous oxide technique. Normal values for blood flow, oxygen utilization, glucose utilization, and peripheral resistance, with observations on the effect of tilting and anxiety. *Journal of Clinical Investigation*, **28**(5 Pt 2), 1163–1171.
- Smith, K. A., Waypa, G. B., & Schumacker, P. T. (2017). Redox signaling during hypoxia in mammalian cells. *Redox Biology*, **13**, 228–234.
- Stamler, J. S., Jia, L. i., Eu, J. P., McMahon, T. J., Demchenko, I. T., Bonaventura, J., Gernert, K., & Piantadosi, C. A. (1997). Blood flow regulation by S-nitrosohemoglobin in the physiological oxygen gradient. *Science*, **276**(5321), 2034–2037.
- Thurnham, D. I., Smith, E., & Flora, P. S. (1988). Concurrent liquid-chromatographic assay of retinol, α -tocopherol, β -carotene, a -carotene, lycopene, and β -cryptoxanthin in plasma, with tocopherol acetate as internal standard. *Clinical Chemistry*, **34**(2), 377–381.
- Turrens, J. F. (2003). Mitochondrial formation of reactive oxygen species. *The Journal of Physiology*, **552**(2), 335–344.
- Vuilleumier, J. P., & Keck, E. (1993). Fluorimetric assay of vitamin C in biological materials using a centrifugal analyser with fluorescence attachment. *Journal of Micro-nutritional Analysis*, **5**, 25–34.
- Wang, J., Brown, M. A., Tarn, S. H., Chan, M. C., & Whitworth, J. A. (1997). Effects of diet on measurement of nitric oxide metabolites. *Clinical and Experimental Pharmacology and Physiology*, **24**(6), 418–420.
- Wang, X., Bryan, N. S., Macarthur, P. H., Rodriguez, J., Gladwin, M. T., & Feilisch, M. (2006). Measurement of nitric oxide levels in the red cell: validation of tri-iodide-based chemiluminescence with acid-sulfanilamide pretreatment. *The Journal of Biological Chemistry*, **281**(37), 26994–27002.
- Wesseling, K. H., Jansen, J. R., Settels, J. J., & Schreuder, J. J. (1993). Computation of aortic flow from pressure in humans using a nonlinear, three-element model. *Journal of Applied Physiology*, **74**(5), 2566–2573.
- Williams, N. h., & Yandell, J. k (1982). Outer-sphere electron-transfer reactions of ascorbic anions. *Australian Journal of Chemistry*, **35**(6), 1133–1144.
- Willie, C. K., Ainslie, P. N., Drvis, I., Macleod, D. B., Bain, A. R., Madden, D., Maslov, P. Z., & Dujic, Z. (2015). Regulation of brain blood flow and oxygen delivery in elite breath-hold divers. *Journal of Cerebral Blood Flow and Metabolism*, **35**(1), 66–73.
- Willie, C. K., Macleod, D. B., Shaw, A. D., Smith, K. J., Tzeng, Y. C., Eves, N. D., Ikeda, K., Graham, J., Lewis, N. C., Day, T. A., & Ainslie, P. N. (2012). Regional brain blood flow in man during acute changes in arterial blood gases. *The Journal of Physiology*, **590**(14), 3261–3275.
- Willie, C. K., Tzeng, Y. u- C., Fisher, J. A., & Ainslie, P. N. (2014). Integrative regulation of human brain blood flow. *The Journal of Physiology*, **592**(5), 841–859.
- WMA (2013). World Medical Association Declaration of Helsinki: Ethical principles for medical research involving human subjects. *Journal of the American Medical Association*, **310**(20), 2191–2194.
- Woodman, R. J., Playford, D. A., Watts, G. F., Cheetham, C., Reed, C., Taylor, R. R., Puddey, I. B., Beilin, L. J., Burke, V., Mori, T. A., & Green, D. (2001). Improved analysis of brachial artery ultrasound using a novel edge-detection software system. *Journal of Applied Physiology*, **91**(2), 929–937.

Wray, D. W., Uberoi, A., Lawrenson, L., Bailey, D. M., & Richardson, R. S. (2009). Oral antioxidants and cardiovascular health in the exercise-trained and untrained elderly: A radically different outcome. *Clinical Science*, **116**(5), 433–441.

Xu, F., Uh, J., Brier, M. R., Hart, J., Yezhuvath, U. S., Gu, H., Yang, Y., & Lu, H. (2011). The influence of carbon dioxide on brain activity and metabolism in conscious humans. *Journal of Cerebral Blood Flow and Metabolism*, **31**(1), 58–67.

Additional information

Data availability statement

Original data arising from this research are available directly from Professor Damian Miles Bailey upon reasonable request.

Competing interests

D.M.B. is Editor-in-Chief of *Experimental Physiology*, Chair of the Life Sciences Working Group, member of the Human Spaceflight and Exploration Science Advisory Committee to the European Space Agency, member of the Space Exploration Advisory Committee to the UK Space Agency, member of the National Cardiovascular Network for Wales and South East Wales Vascular Network and is affiliated to the companies FloTBI, Inc. and Bexorg, Inc. focused on the technological development of novel biomarkers of cerebral bioenergetic function and structural damage in humans.

Author contributions

D.M.B., A.R.B., I.D., D.B.M., Z.D. and P.N.A. conceived and designed the research. D.M.B., A.R.B., R.L.H., O.F.B., I.D., Z.D. and P.N.A. obtained funding. D.M.B., A.R.B., R.L.H., O.F.B., I.D., D.B.M., Z.D. and P.N.A. performed the experiments. D.M.B., A.R.B., R.L.H., O.F.B., I.D., B.S., A.I., G.W.D., R.H.D., R.M.G.B., D.B.M., Z.D. and P.N.A. contributed to data analysis. D.M.B., A.R.B., R.L.H., Z.D. and P.N.A. inter-

preted results of the experiments. D.M.B. drafted the manuscript and revisions thereof. All authors edited and revised the manuscript(s) critically for important intellectual content. All authors approved the final version of the manuscript and agree to be accountable for all aspects of the work in ensuring that questions related to the accuracy or integrity of any part of the work are appropriately investigated and resolved. All persons designated as authors qualify for authorship, and all those who qualify for authorship are listed.

Funding

This study was funded by a Royal Society Wolfson Research Fellowship (#WM170007) and Higher Education Funding Council for Wales (D.M.B.), Canada Research Chair (CRC) and Natural Sciences and Engineering Research Council of Canada (NSERC) Discovery grant (P.N.A.), NSERC (A.R.B. and R.L.H.), Autonomic Province of Vojvodina, Serbia (#142-451-2541, OFB) and Croatian Science Foundation (#IP-2014-09-1937, O.F.B., I.D., Z.D. and P.N.A.).

Acknowledgements

The authors acknowledge the cheerful cooperation of all participants. We are also indebted to Professor I. S. Young and Dr Jane McEneny for specialist technical input.

Keywords

carbon dioxide, cerebral blood flow, free radicals, nitric oxide, oxygen

Supporting information

Additional supporting information can be found online in the Supporting Information section at the end of the HTML view of the article. Supporting information files available:

Peer Review History